Journal of Computational Mathematics
Vol.xx, No.x, 2026, 1–34.

http://www.global-sci.org/jcm
doi:10.4208/jcm.2508-m2024-0257

MULTI-LEVEL MIXED FINITE ELEMENT METHODS BASED ON DIFFERENT ITERATIONS FOR THE STEADY BOUSSINESQ PROBLEM*

Liwei Liu, Tong Zhang and Chuanjun Chen[1)]
School of Mathematics and Information Sciences, Yantai University, Yantai 264005, China
E-mail: cjchen@ytu.edu.cn

Abstract

Three multi-level mixed finite element methods for the steady Boussinesq equations are analyzed and discussed in this paper. The nonlinear and multi-variables coupled problem on a coarse mesh with the mesh size h_0 is solved firstly, and then, a series of decoupled and linear subproblems with the Stokes, Oseen and Newton iterations are solved on the successive and refined grids with the mesh sizes $h_j,\ j = 1, 2, \ldots, J$. The computational scales are reduced and the computational costs are saved. Furthermore, the uniform stability and convergence results in both L^2- and H^1-norms of are derived under some uniqueness conditions by using the mathematical induction and constructing the dual problems. Theoretical results show that the multi-level methods have the same order of numerical solutions in the H^1-norm as the one level method with the mesh sizes $h_j = h_{j-1}^2,\ j = 1, 2, \ldots, J$. Finally, some numerical results are provided to investigate and compare the effectiveness of the multi-level mixed finite element methods.

Mathematics subject classification: 65N10, 65N30, 76Q10.
Key words: Steady Boussinesq problem, Multi-level methods, Stability, Error estimates.

1. Introduction

In this paper, we consider the following steady Boussinesq problem:

$$\begin{cases} -Pr\Delta u + (u\cdot\nabla)u + \nabla p = PrRa\, iT + f & \text{in } \Omega, \\ \nabla\cdot u = 0 & \text{in } \Omega, \\ -\nabla\cdot(k\nabla T) + (u\cdot\nabla)T = g & \text{in } \Omega, \\ u = 0, \quad T = 0 & \text{on } \partial\Omega, \end{cases} \tag{1.1}$$

where $\Omega \subset \mathbb{R}^2$ is a bounded domain with Lipschitz boundary $\partial\Omega$, the notations $u = (u_1(x, y), u_2(x, y))'$, $p = p(x, y), T = T(x, y)$ are the velocity, pressure and temperature fields, the parameters Pr, Ra and k are the Prandtl number, the Rayleigh number and the thermal conductivity parameter, respectively. The letter $i = \binom{0}{1}$ is the unit vector of the gravitational acceleration, f and g are the body forces.

The Boussinesq problem is an important mathematical model, which can be used to describe many phenomenons of the ordinary life and engineering applications. For example, the ventilation and heating, the nuclear reaction systems, the electronic equipment cooling and so

* Received November 20, 2024 / Revised version received June 25, 2025 / Accepted August 13, 2025 / Published online January 13, 2026 /
[1)] Corresponding author

on [3, 4, 8, 15]. Finding the analytical solutions of problem (1.1) is an impossible work due to its inherent characteristics, such as the incompressibility, the nonlinearity and the coupling of multi-variables. Hence, the numerical simulation becomes an important way to understand and study the behaviors of problem (1.1). Many works were published in the recent decades years, for example, Wu [36] considered the existence, uniqueness and smoothness of solutions for problem (1.1) in some special functional spaces. Some new regularity criteria of the weak solutions were provided in [14]. Later, paper [33] established the global existence of the weak solution to the two/three dimensional incompressible Magnetohydrodynamic (MHD) equations and MHD-Boussinesq fluid. For more theoretical findings about problem (1.1), one can refer to [34, 39] and the references therein. In the respect to the numerical analysis, we can refer to the iterative methods [3, 28, 32], the two level methods [28, 41, 45], the projection/splitting schemes [43, 44] and so on. For more numerical methods about problem (1.1), we can refer to [23, 35, 40, 42] and the references therein.

The multi-level method is an efficient numerical scheme for the nonlinear problems, the key idea of this method is to solve the nonlinear problems on the coarse mesh firstly, and then a series of decoupled and linear subproblems are solved on the fine mesh successively. The main feature of multi-level method is that it not only keeps the same convergence rates as the one level method with the mesh sizes satisfy $h_j = h_{j-1}^2$, but also it can save a lot of computational cost. For example, Xu [37, 38] considered the two level method for the elliptic equations and the nonlinear PDEs, the optimal error estimates were obtained as $h = H^2$. Later, the two-level method for the steady Navier-Stokes equations was considered in [18, 20] and the convergence results in H^1-norm were shown under the mesh sizes $h = H^2$, which were extended to the multi-level method [17, 19]. After that, the multi-level method has been widely used to treat various problems, here we just mention [2,7,30] for the elliptic problems, [1,3,5] for the parabolic equations, [13, 19, 21, 22, 27] for the incompressible flows. For more recent developments about the multi-level method, we can refer to [10, 12, 16] and the references therein.

In this paper, we design three multi-level methods based on the Stokes, Oseen and Newton iterations for the steady Boussinesq equations. Compared with the existing works of multi-level methods for the incompressible flows, the novelties of this paper can be listed as follows:

(1) Since there is an unknown T on the right-hand side of problem (1.1), a positive constant $\xi = 2C_0^2 PrRa/k$ needs to be introduced to establish the H^2-stability of numerical schemes. The theoretical analysis requires more techniques, including the mathematical induction and energy method.

(2) The L^2-norm error estimates of numerical solutions of the multi-level methods with different iterations are presented by constructing the duality problems with the mesh sizes satisfying $h_j = h_{j-1}^{3/2}$, which were not provided in the previous works [21,27,28,41]. Furthermore, the optimal error estimates in H^1-norms are also provided with the mesh sizes satisfy $h_j = h_{j-1}^2$, $j = 1, 2, \ldots, J$.

(3) Some numerical results are presented to show the performances of the established theoretical analysis. From these theoretical findings, we see that the multi-level methods have the same H^1-norm accuracy as the one level method, while the multi-level method takes less computational cost.

The rest of this paper is organized as follows. Section 2 recalls some basic notations of the Sobolev spaces and the regularity results of problem (1.1). Section 3 provides the Galerkin

finite element method for the Boussinesq equations and some existed theoretical results. Sections 4-6 present the multi-level method based on the Stokes, Oseen and Newton iterations for the steady Boussinesq equations, the corresponding stability and convergence results of numerical solutions in both L^2- and H^1-norms are developed, respectively. Some numerical results are given in Section 7 to verify the established theoretical findings and show the performances of the considered numerical schemes. Finally, a conclusion is made in Section 8.

2. Preliminaries

For the mathematical setting of problem (1.1), the standard Sobolev spaces and the corresponding norms are used. For example, we set $H^k(\Omega) = W^{k,2}(\Omega)$ for the nonnegative integers k with norm

$$\|v\|_k = \left(\sum_{|\gamma|=0}^{k} \|D^\gamma v\|_0^2 \right)^{\frac{1}{2}}.$$

The inner product is denoted by $(\cdot\,,\cdot)$, that is $(\phi, \varphi) = \int_\Omega \phi\varphi dx$. In order to simplify the notations, the following classical Sobolev spaces are introduced:

$$\begin{aligned}
&X = H_0^1(\Omega)^2 = \{v \in H^1(\Omega)^2 : v = 0 \ \text{ on } \partial\Omega\},\\
&M = L_0^2(\Omega) = \{q \in L^2(\Omega) : (q, 1)_\Omega = 0\},\\
&W = H_0^1 = \{\phi \in H^1(\Omega) : \phi = 0 \ \text{ on } \partial\Omega\},\\
&V = \{v \in X : \nabla \cdot v = 0 \ \text{ in } \Omega\},\\
&Y = L^2(\Omega)^2,\\
&H = \{v \in Y : \nabla \cdot v = 0,\ v \cdot n|_{\partial\Omega} = 0\},\\
&Z = L^2(\Omega),\\
&D(A) = H^2(\Omega)^2 \cap X,\\
&H(A) = H^2(\Omega) \cap W,
\end{aligned}$$

where $A_i = -P_i\Delta,\ i = 1, 2$ with the notation Δ is the Laplace operator and P_i is the L^2-orthogonal projection from Y to V and from Z to W, respectively,

$$\begin{aligned}
&(u - P_1 u, v_h) = 0, \quad \forall\, u \in Y, \quad v \in V,\\
&(\theta - P_2\theta, \psi) = 0, \quad \forall\, \theta \in Z, \quad \psi \in W.
\end{aligned}$$

Define the bilinear forms $a(\cdot\,,\cdot), d(\cdot\,,\cdot)$ and $\overline{a}(\cdot\,,\cdot)$ on $X \times X, X \times M$ and $W \times W$ by

$$\begin{aligned}
&a(u, v) = Pr(\nabla u, \nabla v), \quad d(v, q) = (q, \nabla \cdot v), \quad \forall\, u, v \in X, \quad q \in M,\\
&\overline{a}(T, \psi) = k(\nabla T, \nabla \psi), \qquad\qquad\qquad\quad \forall\, T, \psi \in W,\\
&\|\phi\|_0 \le C_0 \|\nabla \phi\|_0, \qquad\qquad\qquad\quad \forall\, \phi \in X \ \text{ or } \ W,
\end{aligned}$$

here and below, the letter C or with its subscript denotes a generic positive constant independent of the mesh parameter and may be different at its different occurrences.

Moreover, we define the trilinear forms for all $u, v, w \in X$ and $T, \psi \in W$,

$$b(u, v, w) = \big((u \cdot \nabla)v, w\big), \quad \overline{b}(u, T, \psi) = (u \cdot \nabla T, \psi).$$

As mentioned above, some assumptions on the domain Ω are required (see [9, 11, 29]).

Assumption 2.1. Assume that the boundary of Ω is smooth, then the following Stokes problem:

$$-\Delta v + \nabla q = f, \quad \nabla \cdot v = 0 \quad \text{in } \Omega, \quad v = 0 \quad \text{on } \partial\Omega$$

with the function $f \in Y$ has a unique solution, it satisfies

$$\|v\|_2 + \|q\|_1 \le C\|f\|_0,$$

and the following elliptic equation:

$$-\Delta\phi = g \quad \text{in } \Omega, \quad \phi|_{\partial\Omega} = 0$$

with the function $g \in Z$ has a unique solution $\phi \in W$ and it holds

$$\|\phi\|_2 \le C\|g\|_0.$$

With above notations, the variational formulation of problem (1.1) reads as: For all $(v, q, \phi) \in X \times M \times W$, find $(u, p, T) \in X \times M \times W$ such that

$$\begin{aligned} &A\big((u,T),(v,\psi)\big) - d(v,p) + d(u,q) + B\big((u,u),(u,T),(v,\psi)\big) \\ &= PrRa(iT, v) + \langle F, (v,\psi)\rangle, \end{aligned} \tag{2.1}$$

where

$$\begin{aligned} &A\big((u,T),(v,\psi)\big) = a(u,v) + \bar{a}(T,\psi), \\ &\langle F,(v,\psi)\rangle = (f,v) + (g,\psi), \\ &B\big((u,u),(u,T),(v,\psi)\big) = b(u,u,v) + \bar{b}(u,T,\psi). \end{aligned}$$

The following estimates about the linear and trilinear terms can be found in [4,9,17,24,29]:

$$A\big((u,T),(v,\psi)\big) \le \max\{Pr,k\}\|(u,T)\|_1\|(v,\psi)\|_1, \qquad \forall\, u,v \in X,\ T,\psi \in W, \tag{2.2}$$

$$A\big((u,T),(u,T)\big) \ge \min\{Pr,k\}\|(u,T)\|_1^2, \qquad \forall\, u \in X, \quad T \in W, \tag{2.3}$$

$$B\big((u,u),(v,T),(w,\psi)\big) = -B\big((u,u),(w,\psi),(v,T)\big), \quad \forall\, u \in V, \quad v,w \in X,\ T,\psi \in W, \tag{2.4}$$

$$B\big((u,u),(v,T),(v,T)\big) = 0, \qquad \forall\, u \in V, \quad v \in X, \quad T \in W, \tag{2.5}$$

$$\begin{aligned} &\big|B\big((u,u),(u,T),(v,\psi)\big)\big| \\ &\le \max\{N,\bar{N}\}\|(u,u)\|_1\|(u,T)\|_1\|(v,\psi)\|_1, \end{aligned} \qquad \forall\, u,v \in X,\ T,\psi \in W \tag{2.6}$$

with

$$\begin{aligned} &\|(u,T)\|_i^2 = \|u\|_i^2 + \|T\|_i^2, \\ &N = \sup_{u,v,w\in X} \frac{|b(u,v,w)|}{\|\nabla u\|_0\|\nabla v\|_0\|\nabla w\|_0}, \\ &\bar{N} = \sup_{u\in X,\ T,\psi\in W} \frac{|\bar{b}(u,T,\psi)|}{\|\nabla u\|_0\|\nabla T\|_0\|\nabla\psi\|_0}, \end{aligned}$$

and

$$\begin{aligned} &\big|B\big((u,u),(w,T),(v,\psi)\big)\big| \le C_1\|(A_1u, A_1u)\|_0\|(w,T)\|_1\|(v,\psi)\|_0, \\ &\quad \forall\, u \in D(A), \quad w \in X, \quad T \in W, \quad v \in Y, \quad \psi \in Z, \end{aligned} \tag{2.7}$$

$$\begin{aligned} &\big|B\big((u,u),(w,T),(v,\psi)\big)\big| \le C_2\|(u,u)\|_1\|(w,T)\|_1^{\frac{1}{2}}\|(A_1w, A_2T)\|_0^{\frac{1}{2}}\|(v,\psi)\|_0, \\ &\quad \forall\, u \in X, \quad w \in D(A), \quad T \in H(A), \quad v \in Y, \quad \psi \in Z. \end{aligned} \tag{2.8}$$

Theorem 2.1. *Under the Assumption* 2.1*, there exists a constant* $\xi = 2C_0^2 PrRa/k$ *such that*

$$\|(u,T)\|_1 \le \frac{\|F_\xi\|_{-1}}{\min\{Pr, C_0^2 PrRa\}}, \quad \|(A_1u, A_2T)\|_0 \le C(\|F_\xi\|_{-1} + \|F\|_0), \tag{2.9}$$

where

$$\|F_\xi\|_{-1} = \sup_{(0,0)\neq(v,\psi)\in X\times W} \frac{\langle F, (v, \xi\psi)\rangle}{\|(v,\psi)\|_1}.$$

Furthermore, if the parameters $Pr, Ra, N, \bar{N}$ *and* C_0 *satisfies*

$$0 < \sigma = \frac{\max\{N, \xi\bar{N}\}}{\big(\min\{Pr, C_0^2 PrRa\}\big)^2}\|F_\xi\|_{-1} < \frac{1}{2}, \tag{2.10}$$

then, the problem (2.1) *has a unique solution.*

Proof. Choosing $v = u, q = p$ and $\psi = \xi T$ in (2.1), using (2.3) and (2.5), one finds

$$\begin{aligned}
&\min\{Pr, \xi k\}\|(u,T)\|_1^2 \\
&\le A\big((u,T),(u,\xi T)\big) \\
&\le PrRa\|T\|_0\|u\|_0 + \|F_\xi\|_{-1}\|(u,T)\|_1 \\
&\le C_0^2 PrRa\|T\|_1\|(u,T)\|_1 + \|F_\xi\|_{-1}\|(u,T)\|_1.
\end{aligned}$$

Thanks to the choice of ξ, we obtain the first inequality of (2.9).

Next, taking $v = A_1u \in V, q = 0$ and $\psi = A_2T$ in (2.1), using (2.3) and (2.8), we have

$$\begin{aligned}
&\min\{Pr, k\}\|(A_1u, A_2T)\|_0^2 \\
&\le A\big((u,T),(A_1u,A_2T)\big) \\
&\le PrRa\|T\|_0\|A_1u\|_0 + \|F\|_0\|(A_1u,A_2T)\|_0 \\
&\quad + C_2\|(u,u)\|_1\|(u,T)\|_1^{\frac{1}{2}}\|(A_1u,A_2T)\|_0^{\frac{3}{2}} \\
&\le PrRa\|T\|_0\|(A_1u,A_2T)\|_0 + \|F\|_0\|(A_1u,A_2T)\|_0 \\
&\quad + \frac{\min\{Pr,k\}}{2}\|(A_1u,A_2T)\|_0^2 + \frac{C_2^4}{2\min\{Pr,k\}}\|(u,u)\|_1^4\|(u,T)\|_1^2.
\end{aligned}$$

Combining with the bounds of $\|u\|_1$ and $\|(u,T)\|_1$, we obtain (2.9).

Finally, we assume that (u_1, p_1, T_1) and (u_2, p_2, T_2) are the solutions of problem (2.1), then it holds

$$\begin{aligned}
&A\big((u_1-u_2, T_1-T_2),(v,\psi)\big) - d(v, p_1-p_2) \\
&\quad + B\big((u_1-u_2,u_1-u_2),(u_1,T_1),(v,\psi)\big) \\
&\quad + d(u_1-u_2,q) + B\big((u_2,u_2),(u_1-u_2,T_1-T_2),(v,\psi)\big) \\
&= PrRa\big(i(T_1-T_2),v\big).
\end{aligned} \tag{2.11}$$

Taking $v = u_1 - u_2, q = p_1 - p_2, \psi = \xi(T_1 - T_2)$ in (2.11) and using (2.3), (2.5), one finds that

$$\begin{aligned}
&\min\{Pr, \xi k\}\|(u_1-u_2, T_1-T_2)\|_1^2 \\
&\le A\big((u_1-u_2,T_1-T_2),\big(u_1-u_2,\xi(T_1-T_2)\big)\big) \\
&= PrRa\big(i(T_1-T_2),u_1-u_2\big) \\
&\quad - B\big((u_1-u_2,u_1-u_2),(u_1,T_1),\big(u_1-u_2,\xi(T_1-T_2)\big)\big) \\
&\le C_0^2 PrRa\|T_1-T_2\|_1\|(u_1-u_2,T_1-T_2)\|_1 \\
&\quad + \max\{N,\xi\bar{N}\}\|(u_1-u_2,u_1-u_2)\|_1\|(u_1,T_1)\|_1\|(u_1-u_2,T_1-T_2)\|_1.
\end{aligned}$$

With the choice of $\xi = 2C_0^2 PrRa\, k^{-1}$, we arrive at

$$\begin{aligned}
&\|(u_1 - u_2, T_1 - T_2)\|_1 \\
\leq\ & \frac{\max\{N, \xi\bar{N}\}}{\min\{Pr, C_0^2 PrRa\}} \|(u_1, T_1)\|_1 \|(u_1 - u_2, u_1 - u_2)\|_1 \\
\leq\ & \frac{\max\{N, \xi\bar{N}\}}{(\min\{Pr, C_0^2 PrRa\})^2} \|F_\xi\|_{-1} \|(u_1 - u_2, u_1 - u_2)\|_1.
\end{aligned}$$

Thanks to (2.9) and (2.10), we obtain that $\|(u_1 - u_2, T_1 - T_2)\|_1 = 0$, it means that $u_1 = u_2$ and $T_1 = T_2$. Hence, the problem (2.1) admits a unique solution. □

3. Mixed Finite Element Method

Let K_λ be a regular, quasi-uniform partition of the domain Ω with the largest element diameter of $\lambda = h_0, h_1, \ldots, h_J$ and $h_0 > h_1 > \cdots > h_J$. The notation K_{h_j} is the finer partition generated from the previous partition $K_{h_{j-1}}$. In this paper, we choose the following finite element spaces:

$$\begin{aligned}
X_\lambda &= \{v \in C^0(\bar{\Omega})^2 \cap X;\ v|_K \in P_{1b}(K)^2,\ \forall\, K \in K_\lambda\}, \\
M_\lambda &= \{q \in C^0(\bar{\Omega}) \cap M;\ q|_K \in P_1(K),\ \forall\, K \in K_\lambda\}, \\
W_\lambda &= \{\psi \in C^0(\bar{\Omega}) \cap W;\ \psi|_K \in P_1(K),\ \forall\, K \in K_\lambda\},
\end{aligned}$$

where

$$P_{1b}(K) = \{v_\lambda \in C^0(\bar{\Omega}); v_\lambda|_K \in P_1(K) \oplus \mathrm{span}\{\hat{b}\}, K \in K_\lambda\},$$

and $\hat{b}$ is the bubble function, $P_1(K)$ is the set of linear polynomials on the element $K \in K_\lambda$.

It is well-known that the above finite element spaces X_h and M_h satisfies (see [9, 29])

$$\beta\|q_h\|_0 \leq \inf_{q_h \in M_h} \sup_{v_h \in X_h} \frac{d(v_h, q_h)}{\|\nabla v_h\|_0}, \tag{3.1}$$

where $\beta > 0$ is a constant.

Define the discrete finite element space V_λ

$$V_\lambda = \{v_\lambda \in X_\lambda;\ d(v_\lambda, q_\lambda) = 0,\ \forall\, q_\lambda \in M_\lambda\}.$$

Introducing two L^2-orthogonal projections $P_{1\lambda} : Y \to V_\lambda$ and $P_{2\lambda} : Z \to W_\lambda$ by

$$\begin{aligned}
&(u - P_{1\lambda}u, v_h) = 0, \quad \forall\, u \in Y, \quad v \in V_\lambda, \\
&(\theta - P_{2\lambda}\theta, \psi_h) = 0, \quad \forall\, \theta \in Z, \quad \psi_h \in W_\lambda.
\end{aligned}$$

Define the discrete Stokes operator $A_{1\lambda} = -P_{1\lambda}\Delta_\lambda$ and the elliptic operator $A_{2\lambda} = -P_{2\lambda}\Delta_\lambda$, where Δ_λ is given by

$$(-\Delta_\lambda\phi_\lambda, \varphi_\lambda) = (\nabla\phi_\lambda, \nabla\varphi_\lambda), \quad \forall\, \phi_\lambda, \varphi_\lambda \in X_\lambda \text{ or } W_\lambda$$

with the discrete norms $\|\phi_\lambda\|_{k,\lambda} = \|A_{i\lambda}^{k/2}\phi_\lambda\|_0$ for $i = 1, 2,\ k = 0, 1, 2$.

The following projections are classical, which can be found in [4, 9, 24, 29]:

(1) The Stokes projection. For all $(v_\lambda, q_\lambda) \in X_\lambda \times M_\lambda$, find $(R_\lambda(u,p), Q_\lambda(u,p)) \in X_\lambda \times M_\lambda$ such that

$$a\big(u - R_\lambda(u,p), v_\lambda\big) - d\big(v_\lambda, p - Q_\lambda(u,p)\big) + d\big(u - R_\lambda(u,p), q_\lambda\big) = 0.$$

Then, it holds

$$\|u - R_\lambda(u,p)\|_0 + \lambda\big(\big\|\nabla\big(u - R_\lambda(u,p)\big)\big\|_0 + \|p - Q_\lambda(u,p)\|_0\big) \le C\lambda^2(\|u\|_2 + \|p\|_1). \tag{3.2}$$

(2) The elliptic projection. For all $\phi \in W_\lambda$, find $\widetilde{P}_\lambda T \in W_\lambda$ such that

$$\big(\nabla(\widetilde{P}_\lambda T - T), \nabla\phi_\lambda\big) = 0.$$

Then, we have

$$\|T - \widetilde{P}_\lambda T\|_0 + \lambda\|\nabla(T - \widetilde{P}_\lambda T)\|_1 \le C\lambda^2\|T\|_2, \quad \forall\, T \in H(A). \tag{3.3}$$

The Galerkin mixed finite element method for problem (2.1) reads as: For all $(v_\lambda, q_\lambda, \psi_\lambda) \in X_h \times M_h \times W_h$, find $(u_\lambda, p_\lambda, T_\lambda) \in X_h \times M_h \times W_h$ such that

$$\begin{aligned} &A\big((u_\lambda, T_\lambda), (v_\lambda, \psi_\lambda)\big) - d(v_\lambda, p_\lambda) + d(u_\lambda, q_\lambda) + B\big((u_\lambda, u_\lambda), (u_\lambda, T_\lambda), (v_\lambda, \psi_\lambda)\big) \\ &= PrRa(iT_\lambda, v_\lambda) + \langle F, (v_\lambda, \psi_\lambda)\rangle. \end{aligned} \tag{3.4}$$

By using the same tricks as employed in Theorem 2.1, the following results hold.

Theorem 3.1 (See [42, 45]). *Under the assumptions of Theorem* 2.1*, the problem* (3.4) *has a unique solution* $(u_\lambda, p_\lambda, T_\lambda)$ *and satisfies*

$$\begin{aligned} &\|(u_\lambda, T_\lambda)\|_1 \le \frac{\|F_\xi\|_{-1}}{\min\{Pr, C_0^2 PrRa\}}, \\ &\|(A_{1\lambda}u_\lambda, A_{2\lambda}T_\lambda)\|_0 \le C(\|F_\xi\|_{-1} + \|F\|_0), \\ &\|u - u_\lambda\|_0 + \|T - T_\lambda\|_0 + \lambda(\|u - u_\lambda\|_1 + \|T - T_\lambda\|_1 + \|p - p_\lambda\|_0) \le C\lambda^2. \end{aligned}$$

4. Multi-level Method Based on the Stokes Iteration

The following sections focus on the multi-level methods with different iterations. Let $K_{h_0}, K_{h_1}, \ldots, K_{h_J}$ be the partitions of the domain Ω, the finite element spaces X_{h_j}, M_{h_j} and W_{h_j} with $j = 0, 1, \ldots, J$ satisfy

$$(X_{h_0}, M_{h_0}, W_{h_0}) \subset (X_{h_1}, M_{h_1}, W_{h_1}) \subset \cdots \subset (X_{h_J}, M_{h_J}, W_{h_J}).$$

Firstly, we consider the multi-level method based on the Stokes iteration for problem (2.1) (Algorithm 4.1).

Theorem 4.1. *Under the assumptions of Theorem* 2.1 *and* $0 < \sigma \le 1/8$*, the numerical solutions* u_{h_j} *and* T_{h_j} *of problem* (4.2) *satisfy*

$$\begin{aligned} &\|(u_{h_j}, T_{h_j})\|_1 \le \frac{6}{5}\frac{\|F_\xi\|_{-1}}{\min\{Pr, C_0^2 PrRa\}}, \\ &\|(A_{1h}u_{h_j}, A_{2h}T_{h_j})\|_0 \le C(\|F_\xi\|_{-1} + \|F\|_0). \end{aligned} \tag{4.3}$$

Algorithm 4.1: Multi-Level Method Based on the Stokes Iteration.

Step I: *Solve the nonlinear problem (3.4) on a coarse mesh K_{h_0}, i.e., for all $(v_{h_0}, q_{h_0}, \psi_{h_0}) \in X_{h_0} \times M_{h_0} \times W_{h_0}$, find $(u_{h_0}, p_{h_0}, T_{h_0}) \in X_{h_0} \times M_{h_0} \times W_{h_0}$ such that

$$\begin{aligned} &A\big((u_{h_0}, T_{h_0}), (v_{h_0}, \psi_{h_0})\big) - d(v_{h_0}, p_{h_0}) + d(u_{h_0}, q_{h_0}) \\ &\quad + B\big((u_{h_0}, u_{h_0}), (u_{h_0}, T_{h_0}), (v_{h_0}, \psi_{h_0})\big) \\ &= PrRa(iT_{h_0}, v_{h_0}) + \langle F, (v_{h_0}, \psi_{h_0})\rangle. \end{aligned} \tag{4.1}$$

Step II: *Solve the linearized problem based on the Stokes iteration on the mesh K_{h_j} successively, i.e., for all $(v_{h_j}, q_{h_j}, \psi_{h_j}) \in X_{h_j} \times M_{h_j} \times W_{h_j}$, find $(u_{h_j}, p_{h_j}, T_{h_j}) \in X_{h_j} \times M_{h_j} \times W_{h_j}$ with $j = 1, 2, \ldots, J$ such as

$$\begin{aligned} &A\big((u_{h_j}, T_{h_j}), (v_{h_j}, \psi_{h_j})\big) - d(v_{h_j}, p_{h_j}) + d(u_{h_j}, q_{h_j}) \\ &\quad + B\big((u_{h_{j-1}}, u_{h_{j-1}}), (u_{h_{j-1}}, T_{h_{j-1}}), (v_{h_j}, \psi_{h_j})\big) \\ &= PrRa(iT_{h_j}, v_{h_j}) + \langle F, (v_{h_j}, \psi_{h_j})\rangle. \end{aligned} \tag{4.2}$$

Proof. We prove it by the mathematical induction. Based on Theorem 3.1, one knows that (4.3) holds with $j = 0$. Assume that (4.3) holds with $j = m - 1$, we want to prove it with $j = m$.

Choosing $(v_{h_m}, q_{h_m}, \psi_{h_m}) = (u_{h_m}, p_{h_m}, \xi T_{h_m})$ in (4.2) and using (2.3), (2.5), (2.6), one finds that

$$\begin{aligned} &\min\{Pr, \xi k\}\|(u_{h_m}, T_{h_m})\|_1^2 \\ &\le A\big((u_{h_m}, T_{h_m}), (u_{h_m}, \xi T_{h_m})\big) \\ &= PrRa(iT_{h_m}, u_{h_m}) + \langle F, (u_{h_m}, \xi T_{h_m})\rangle \\ &\quad - B\big((u_{h_{m-1}}, u_{h_{m-1}}), (u_{h_{m-1}}, T_{h_{m-1}}), (u_{h_m}, \xi T_{h_m})\big) \\ &\le C_0^2 PrRa\|T_{h_m}\|_1\|(u_{h_m}, T_{h_m})\|_1 + \|F_\xi\|_{-1}\|(u_{h_m}, T_{h_m})\|_1 \\ &\quad + \max\{N, \xi\bar{N}\}\|(u_{h_{m-1}}, u_{h_{m-1}})\|_1\|(u_{h_{m-1}}, T_{h_{m-1}})\|_1\|(u_{h_m}, T_{h_m})\|_1. \end{aligned}$$

Thanks to the induction assumptions of $\|(u_{h_{m-1}}, T_{h_{m-1}})\|_1$ and $0 < \sigma \le 1/8$, we have

$$\begin{aligned} &\min\big\{Pr, C_0^2 PrRa\big\}\|(u_{h_m}, T_{h_m})\|_1 \\ &\le \|F_\xi\|_{-1} + \frac{36}{25}\frac{\max\{N, \xi\bar{N}\}}{\big(\min\big\{Pr, C_0^2 PrRa\big\}\big)^2}\|F_\xi\|_{-1}^2 \\ &\le \left(1 + \frac{36}{25}\frac{\max\{N, \xi\bar{N}\}}{\big(\min\big\{Pr, C_0^2 PrRa\big\}\big)^2}\|F_\xi\|_{-1}\right)\|F_\xi\|_{-1} \\ &\le \frac{59}{50}\|F_\xi\|_{-1} < \frac{6}{5}\|F_\xi\|_{-1}. \end{aligned} \tag{4.4}$$

Next, taking $v_{h_m} = A_{1h_m}u_{h_m}, q_{h_m} = 0, \psi_{h_m} = A_{2h_m}T_{h_m}$ in (4.2) and using (2.3), (2.8), one gets

$$\begin{aligned} &\min\{Pr, k\}\|(A_{1h_m}u_{h_m}, A_{2h_m}T_{h_m})\|_0^2 \\ &\le A\big((u_{h_m}, T_{h_m}), (A_{1h_m}u_{h_m}, A_{2h_m}T_{h_m})\big) \end{aligned}$$

$$
\begin{aligned}
&= PrRa(iT_{h_m}, A_{1h_m}u_{h_m}) + \langle F, (A_{1h_m}u_{h_m}, A_{2h_m}T_{h_m})\rangle \\
&\quad - B\big((u_{h_{m-1}}, u_{h_{m-1}}), (u_{h_{m-1}}, T_{h_{m-1}}), (A_{1h_m}u_{h_m}, A_{2h_m}T_{h_m})\big) \\
&\le PrRa\|T_{h_m}\|_0\|(A_{1h_m}u_{h_m}, A_{2h_m}T_{h_m})\|_0 + \|F\|_0\|(A_{1h_m}u_{h_m}, A_{2h_m}T_{h_m})\|_0 \\
&\quad + C_2\|(u_{h_{m-1}}, u_{h_{m-1}})\|_1\|(u_{h_{m-1}}, T_{h_{m-1}})\|_1^{\frac{1}{2}}\|(A_{1h_{m-1}}u_{h_{m-1}}, A_{2h_{m-1}}T_{h_{m-1}})\|_0^{\frac{1}{2}} \\
&\quad \times \|(A_{1h_m}u_{h_m}, A_{2h_m}T_{h_m})\|_0.
\end{aligned}
$$

So, we have

$$
\begin{aligned}
&\min\{Pr, k\}\|(A_{1h_m}u_{h_m}, A_{2h_m}T_{h_m})\|_0 \\
&\le PrRa\|T_{h_m}\|_0 + \|F\|_0 + C_2\|(u_{h_{m-1}}, u_{h_{m-1}})\|_1\|(u_{h_{m-1}}, T_{h_{m-1}})\|_1^{\frac{1}{2}} \\
&\quad \times \|(A_{1h_{m-1}}u_{h_{m-1}}, A_{2h_{m-1}}T_{h_{m-1}})\|_0^{\frac{1}{2}}.
\end{aligned}
$$

If

$$
\|(A_{1h_m}u_{h_m}, A_{2h_m}T_{h_m})\|_0 \le \|(A_{1h_{m-1}}u_{h_{m-1}}, A_{2h_{m-1}}T_{h_{m-1}})\|_0,
$$

by the induction assumption, we get

$$
\|(A_{1h_m}u_{h_m}, A_{2h_m}T_{h_m})\|_0 \le C(\|F_\xi\|_{-1} + \|F\|_0).
$$

If

$$
\|(A_{1h_m}u_{h_m}, A_{2h_m}T_{h_m})\|_0 \ge \|(A_{1h_{m-1}}u_{h_{m-1}}, A_{2h_{m-1}}T_{h_{m-1}})\|_0,
$$

one finds that

$$
\begin{aligned}
&\min\{Pr, k\}\|(A_{1h_m}u_{h_m}, A_{2h_m}T_{h_m})\|_0 \\
&\le PrRa\|T_{h_m}\|_0 + \|F\|_0 + C_2\|(u_{h_{m-1}}, u_{h_{m-1}})\|_1\|(u_{h_{m-1}}, T_{h_{m-1}})\|_1^{\frac{1}{2}} \\
&\quad \times \|(A_{1h_{m-1}}u_{h_{m-1}}, A_{2h_{m-1}}T_{h_{m-1}})\|_0^{\frac{1}{2}} \\
&\le C_0PrRa\|T_{h_m}\|_1 + \|F\|_0 + C_2\|(u_{h_{m-1}}, u_{h_{m-1}})\|_1\|(u_{h_{m-1}}, T_{h_{m-1}})\|_1^{\frac{1}{2}} \\
&\quad \times \|(A_{1h_m}u_{h_m}, A_{2h_m}T_{h_m})\|_0^{\frac{1}{2}} \\
&\le C_0PrRa\|T_{h_m}\|_1 + \|F\|_0 + \frac{C_2^2}{2\min\{Pr, k\}}\|(u_{h_{m-1}}, u_{h_{m-1}})\|_1^2\|(u_{h_{m-1}}, T_{h_{m-1}})\|_1 \\
&\quad + \frac{\min\{Pr, k\}}{2}\|(A_{1h_m}u_{h_m}, A_{2h_m}T_{h_m})\|_0. \qquad (4.5)
\end{aligned}
$$

Combining (4.5) with (4.4), we complete the proof. □

Theorem 4.2. *Under the assumptions of Theorem* 4.1*, the numerical solution* (u_{h_1}, T_{h_1}) *of problem* (4.2) *on the mesh* K_{h_1} *satisfies*

$$
\|(u - u_{h_1}, T - T_{h_1})\|_1 + \|p - p_{h_1}\|_0 \le C\big(h_1 + h_0^2\big).
$$

Proof. For all $(v_{h_1}, q_{h_1}, \psi_{h_1}) \in X_{h_1} \times M_{h_1} \times W_{h_1}$, the following error equation holds:

$$
\begin{aligned}
&A\big((u - u_{h_1}, T - T_{h_1}), (v_{h_1}, \psi_{h_1})\big) - d(v_{h_1}, p - p_{h_1}) \\
&\quad + B\big((u, u), (u, T), (v_{h_1}, \psi_{h_1})\big) + d(u - u_{h_1}, q_{h_1}) \\
&\quad - B\big((u_{h_0}, u_{h_0}), (u_{h_0}, T_{h_0}), (v_{h_1}, \psi_{h_1})\big) \\
&= PrRa\big(i(T - T_{h_1}), v_{h_1}\big). \qquad (4.6)
\end{aligned}
$$

Taking $v_{h_1} = R_{h_1}(u,p) - u_{h_1}, q_{h_1} = Q_{h_1}(u,p) - p_{h_1}, \psi_{h_1} = \xi(\widetilde{P}_{h_1}T - T_{h_1})$ in (4.6), applying the Stokes projection, the elliptic projection and (2.7), one finds that

$$\begin{aligned}
&\min\{Pr, \xi k\}\big\|\big(R_{h_1}(u,p) - u_{h_1}, \widetilde{P}_{h_1}T - T_{h_1}\big)\big\|_1^2 \\
&\le A\big(\big(R_{h_1}(u,p) - u_{h_1}, \widetilde{P}_{h_1}T - T_{h_1}\big), \big(R_{h_1}(u,p) - u_{h_1}, \xi(\widetilde{P}_{h_1}T - T_{h_1})\big)\big) \\
&= PrRa\big(i(T - T_{h_1}), R_{h_1}(u,p) - u_{h_1}\big) \\
&\quad - B\big((u - u_{h_0}, u - u_{h_0}), (u,T), \big(R_{h_1}(u,p) - u_{h_1}, \xi(\widetilde{P}_{h_1}T - T_{h_1})\big)\big) \\
&\quad - B\big((u_{h_0}, u_{h_0}), (u - u_{h_0}, T - T_{h_0}), \big(R_{h_1}(u,p) - u_{h_1}, \xi(\widetilde{P}_{h_1}T - T_{h_1})\big)\big) \\
&\le C_0^2 PrRa(\|T - \widetilde{P}_{h_1}T\|_1 + \|\widetilde{P}_{h_1}T - T_{h_1}\|_1)\big\|\big(R_{h_1}(u,p) - u_{h_1}, \widetilde{P}_{h_1}T - T_{h_1}\big)\big\|_1 \\
&\quad + C_1\xi\|(u - u_{h_0}, u - u_{h_0})\|_0\|(A_1u, A_2T)\|_0\big\|\big(R_{h_1}(u,p) - u_{h_1}, \widetilde{P}_{h_1}T - T_{h_1}\big)\big\|_1 \\
&\quad + C_1\xi\|(A_{1h_0}u_{h_0}, A_{1h_0}u_{h_0})\|_0\|(u - u_{h_0}, T - T_{h_0})\|_0\big\|\big(R_{h_1}(u,p) - u_{h_1}, \widetilde{P}_{h_1}T - T_{h_1}\big)\big\|_1.
\end{aligned}$$

As a consequence, thanks to the choice of ξ, (3.3) and Theorem 3.1, we arrive at

$$\min\big\{Pr, C_0^2 PrRa\big\}\big\|\big(R_{h_1}(u,p) - u_{h_1}, \widetilde{P}_{h_1}T - T_{h_1}\big)\big\|_1 \le C\big(h_1 + h_0^2\big).$$

Combining the triangular inequality with the discrete inf-sup condition (3.1), we complete the proof. □

Theorem 4.3. *Under the assumptions of Theorem* 4.1*, the numerical solution* (u_{h_1}, T_{h_1}) *of problem* (4.2) *on the mesh* K_{h_1} *satisfies*

$$\|(u - u_{h_1}, T - T_{h_1})\|_0 \le C\big(h_1^2 + h_1h_0\big).$$

Proof. Find $(\phi, \theta, \varphi) \in X \times M \times W$ for all $(w, r, s) \in X \times M \times W$ such that

$$\begin{aligned}
&A\big((\phi,\varphi),(w,s)\big) + d(w,\theta) - d(\phi,r) + B\big((u_{h_0},u_{h_0}),(w,s),(\phi,\varphi)\big) \\
&\quad + B\big((w,w),(u,T),(\phi,\varphi)\big) - PrRa(is,\phi) = \langle\widetilde{F},(w,s)\rangle.
\end{aligned} \tag{4.7}$$

Since (u,T) is a nonsingular solution, (ϕ,θ,φ) exists uniquely. The assumption that the linearized adjoint problem (4.7) is H^2-regular means that, for all $\widetilde{F} = (\widetilde{f},\widetilde{g}) \in L^2(\Omega)^2 \times L^2(\Omega)$, there is a solution (ϕ,θ,φ) belonging to $H_0^1(\Omega)^2 \cap H^2(\Omega)^2 \times L_0^2(\Omega) \cap H^1 \times H_0^1(\Omega) \cap H^2(\Omega)$ and the following inequality holds:

$$\|(\phi,\varphi)\|_2 + \|\theta\|_1 \le C\|\widetilde{F}\|_0. \tag{4.8}$$

Setting $\widetilde{F} = (u - u_{h_1}, T - T_{h_1})$ and choosing $(w,r,s) = (u - u_{h_1}, p - p_{h_1}, T - T_{h_1})$ in (4.7), it gives

$$\begin{aligned}
&\|(u - u_{h_1}, T - T_{h_1})\|_0^2 \\
&= A\big((\phi,\varphi),(u - u_{h_1}, T - T_{h_1})\big) + d(u - u_{h_1},\theta) \\
&\quad + B\big((u_{h_0},u_{h_0}),(u - u_{h_1}, T - T_{h_1}),(\phi,\varphi)\big) \\
&\quad - d(\phi, p - p_{h_1}) + B\big((u - u_{h_1}, u - u_{h_1}),(u,T),(\phi,\varphi)\big) \\
&\quad - PrRa\big(i(T - T_{h_1}),\phi\big).
\end{aligned}$$

Taking into account the error equation (4.6) and choosing $(v_{h_1}, q_{h_1}, \psi_{h_1}) \in X_{h_1} \times M_{h_1} \times W_{h_1}$, we have

$$\begin{aligned}
&\|(u-u_{h_1}, T-T_{h_1})\|_0^2 \\
&= A\big((u-u_{h_1}, T-T_{h_1}), (\phi - v_{h_1}, \varphi - \psi_{h_1})\big) \\
&\quad + d(u-u_{h_1}, \theta - q_{h_1}) - d(\phi - v_{h_1}, p - p_{h_1}) \\
&\quad + B\big((u_{h_0}, u_{h_0}), (u-u_{h_0}, T-T_{h_0}), (\phi - v_{h_1}, \varphi - \psi_{h_1})\big) \\
&\quad + B\big((u-u_{h_0}, u-u_{h_0}), (u, T), (\phi - v_{h_1}, \varphi - \psi_{h_1})\big) \\
&\quad - PrRa\big(i(T-T_{h_1}), \phi - v_{h_1}\big) \\
&\quad + \underbrace{B\big((u_{h_0}, u_{h_0}), (u_{h_0}-u_{h_1}, T_{h_0}-T_{h_1}), (\phi, \varphi)\big)}_{Term\ I} \\
&\quad + \underbrace{B\big((u_{h_0}-u_{h_1}, u_{h_0}-u_{h_1}), (u, T), (\phi, \varphi)\big)}_{Term\ II}.
\end{aligned}$$

Using (2.4) and (2.7), introducing

$$\overline{\chi} = \frac{1}{|\Omega|}\int_\Omega \chi dx,$$

which is the averages of χ on the domain Ω, one finds

$$\begin{aligned}
&\big|B\big((u_{h_0}, u_{h_0}), (u_{h_0}-u_{h_1}, T_{h_0}-T_{h_1}), (\phi, \varphi)\big)\big| \\
&= \big| - B\big((u_{h_0}, u_{h_0}), (\phi, \varphi), (u_{h_0}-u_{h_1}, T_{h_0}-T_{h_1})\big)\big| \\
&= \big| - \big(u_{h_0}\cdot\nabla(\phi - \overline{\phi}), u_{h_0}-u_{h_1}\big) - \big(u_{h_0}\cdot\nabla(\varphi - \overline{\varphi}), T_{h_0}-T_{h_1}\big)\big| \\
&= \big| - B\big((u_{h_0}, u_{h_0}), (\phi - \overline{\phi}, \varphi - \overline{\varphi}), (u_{h_0}-u_{h_1}, T_{h_0}-T_{h_1})\big)\big| \\
&\le C_1\|(u_{h_0}, u_{h_0})\|_2\|(\phi - \overline{\phi}, \varphi - \overline{\varphi})\|_0\|(u_{h_0}-u_{h_1}, T_{h_0}-T_{h_1})\|_1 \\
&\le Ch_1\big(\|(u_{h_0}-u, T_{h_0}-T)\|_1 + \|(u-u_{h_1}, T-T_{h_1})\|_1\big)\|(\phi, \varphi)\|_1 \\
&\le C\big(h_1^2 + h_1h_0\big)\|(\phi, \varphi)\|_2. \qquad (4.9)
\end{aligned}$$

Similarly, we have

$$\begin{aligned}
&\big|B\big((u_{h_0}-u_{h_1}, u_{h_0}-u_{h_1}), (u, T), (\phi, \varphi)\big)\big| \\
&\le C_1\|(\phi, \varphi)\|_2\|(u-\overline{u}, T-\overline{T})\|_0\|(u_{h_0}-u_{h_1}, T_{h_0}-T_{h_1})\|_1 \\
&\le C\big(h_1^2 + h_1h_0\big)\|(\phi, \varphi)\|_2.
\end{aligned}$$

Taking $v_{h_1} = I_{h_1}\phi, q_{h_1} = \Pi_{h_1}\theta, \psi_{h_1} = J_{h_1}\varphi$ with I_{h_j}, Π_{h_j} and $J_{h_j},\ j = 1, 2, \ldots$ are the standard interpolations in X_{h_1}, M_{h_1} and W_{h_1}, respectively (see [4, 9, 29]), it holds that

$$\begin{aligned}
&\|(u-u_{h_1}, T-T_{h_1})\|_0^2 \\
&\le \max\{Pr, k\}\|(u-u_{h_1}, T-T_{h_1})\|_1\|(\phi - I_{h_1}\phi, \varphi - J_{h_1}\varphi)\|_1 \\
&\quad + \|u-u_{h_1}\|_1\|\theta - \Pi_{h_1}\theta\|_0 + \|p-p_{h_1}\|_0\|\phi - I_{h_1}\phi\|_1 + PrRa\|(T-T_{h_1}, \phi - I_{h_1}\phi)\|_0 \\
&\quad + C_1\|(A_{1h_0}u_{h_0}, A_{1h_0}u_{h_0})\|_0\|(u-u_{h_0}, T-T_{h_0})\|_0\|(\phi - I_{h_1}\phi, \varphi - J_{h_1}\varphi)\|_1 \\
&\quad + C_1\|(u-u_{h_0}, u-u_{h_0}\|_0\|(u, T)\|_2\|(\phi - v_{h_1}, \varphi - \psi_{h_1})\|_1 + C\big(h_1^2 + h_1h_0\big)\|(\phi, \varphi)\|_2 \\
&\le C\big(h_1^2 + h_1h_0\big)(\|(\phi, \varphi)\|_2 + \|\theta\|_1).
\end{aligned}$$

With the help of (4.8) and the choice of $\widetilde{F}$, we complete the proof. □

Remark 4.1. From Theorem 4.2, one knows that the convergence rates of numerical solutions in H^1-norm of two-level method have the same accuracy as the mesh sizes satisfy $h_1 = h_0^2$. Taking $h_0 = \sqrt{h_1}$ in mind, we obtain the L^2-error estimates of numerical solutions u_{h_1} and T_{h_1} from Theorem 4.3, i.e.

$$\|(u - u_{h_1}, T - T_{h_1})\|_0 \le Ch_1^{\frac{3}{2}}.$$

Theorem 4.4. *Under the assumptions of Theorem* 4.1*, the numerical solution* $(u_{h_2}, p_{h_2}, T_{h_2})$ *of problem* (4.2) *on the mesh* K_{h_2} *satisfies*

$$\begin{aligned} &\|(u - u_{h_2}, T - T_{h_2})\|_1 + \|p - p_{h_2}\|_0 \le C\big(h_2 + h_1^{\frac{3}{2}}\big) \simeq Ch_2, \quad h_2 = \mathcal{O}\big(h_1^{\frac{3}{2}}\big), \\ &\|(u - u_{h_2}, T - T_{h_2})\|_0 \le C\big(h_2^2 + h_2h_1\big) \simeq Ch_2^{\frac{3}{2}}, \qquad\qquad h_2 = \mathcal{O}\big(h_1^2\big). \end{aligned} \tag{4.10}$$

Proof. For $j = 2$ and all $(v_{h_2}, q_{h_2}, \psi_{h_2}) \in X_{h_2} \times M_{h_2} \times W_{h_2}$, the following error equation holds:

$$\begin{aligned} &A\big((u - u_{h_2}, T - T_{h_2}), (v_{h_2}, \psi_{h_2})\big) - d(v_{h_2}, p - p_{h_2}) \\ &\quad + B\big((u - u_{h_1}, u - u_{h_1}), (u, T), (v_{h_2}, \psi_{h_2})\big) \\ &\quad + d(u - u_{h_2}, q_{h_2}) + B\big((u_{h_1}, u_{h_1}), (u - u_{h_1}, T - T_{h_1}), (v_{h_2}, \psi_{h_2})\big) \\ &= PrRa\big(i(T - T_{h_2}), v_{h_2}\big). \end{aligned} \tag{4.11}$$

Taking $v_{h_2} = R_{h_2}(u, p) - u_{h_2}, q_{h_2} = Q_{h_2}(u, p) - p_{h_2}, \psi_{h_2} = \xi(\widetilde{P}_{h_2}T - T_{h_2})$ in (4.11), applying the Stokes projection, the elliptic projection and (2.7), one finds that

$$\begin{aligned} &\min\{Pr, \xi k\}\big\|\big(R_{h_2}(u, p) - u_{h_2}, \widetilde{P}_{h_2}T - T_{h_2}\big)\big\|_1^2 \\ &\le A\big(\big(R_{h_2}(u, p) - u_{h_2}, \widetilde{P}_{h_2}T - T_{h_2}\big), \big(R_{h_2}(u, p) - u_{h_2}, \xi(\widetilde{P}_{h_2}T - T_{h_2})\big)\big) \\ &= PrRa\big(i(T - T_{h_2}), R_{h_2}(u, p) - u_{h_2}\big) \\ &\quad - B\big((u - u_{h_1}, u - u_{h_1}), (u, T), \big(R_{h_2}(u, p) - u_{h_2}, \xi(\widetilde{P}_{h_2}T - T_{h_2})\big)\big) \\ &\quad - B\big((u_{h_1}, u_{h_1}), (u - u_{h_1}, T - T_{h_1}), \big(R_{h_2}(u, p) - u_{h_2}, \xi(\widetilde{P}_{h_2}T - T_{h_2})\big)\big) \\ &\le C_0^2 PrRa(\|T - \widetilde{P}_{h_2}T\|_1 + \|\widetilde{P}_{h_2}T - T_{h_2}\|_1)\big\|\big(R_{h_2}(u, p) - u_{h_2}, \widetilde{P}_{h_2}T - T_{h_2}\big)\big\|_1 \\ &\quad + C_1\xi\|(u - u_{h_1}, u - u_{h_1})\|_0\|(A_1u, A_2T)\|_0\big\|\big(R_{h_2}(u, p) - u_{h_2}, \widetilde{P}_{h_2}T - T_{h_2}\big)\big\|_1 \\ &\quad + C_1\xi\|(A_{1h_1}u_{h_1}, A_{1h_1}u_{h_1})\|_0\|(u - u_{h_1}, T - T_{h_1})\|_0\big\|\big(R_{h_2}(u, p) - u_{h_2}, \widetilde{P}_{h_2}T - T_{h_2}\big)\big\|_1. \end{aligned}$$

As a consequence, with the choice of ξ, (3.3) and Theorems 3.1, 4.2 and 4.3, we arrive at

$$\min\big\{Pr, C_0^2 PrRa\big\}\big\|\big(R_{h_1}(u, p) - u_{h_1}, \widetilde{P}_{h_1}T - T_{h_1}\big)\big\|_1 \le C\big(h_2 + h_1^{\frac{3}{2}}\big).$$

Thanks to the triangular inequality and the discrete inf-sup condition (3.1), we obtain (4.10).

Next, choosing $\widetilde{F} = (u - u_{h_2}, T - T_{h_2})$ and $(w, r, s) = (u - u_{h_2}, p - p_{h_2}, T - T_{h_2})$ in (4.7) and replacing u_{h_0} with u_{h_1}, it gives

$$\begin{aligned} &\|(u - u_{h_2}, T - T_{h_2})\|_0^2 \\ &= A\big((\phi, \varphi), (u - u_{h_2}, T - T_{h_2})\big) + d(u - u_{h_2}, \theta) \\ &\quad + B\big((u_{h_1}, u_{h_1})(u - u_{h_2}, T - T_{h_2})(\phi, \varphi)\big) \\ &\quad - d(\phi, p - p_{h_2}) + B\big((u - u_{h_2}, u - u_{h_2}), (u, T), (\phi, \varphi)\big) \\ &\quad - PrRa\big(i(T - T_{h_2}), \phi\big). \end{aligned}$$

Combining the error equation (4.11) with the choice of $(v_{h_2}, q_{h_2}, \psi_{h_2})$ and (4.9), we obtain

$$\begin{aligned}
&\|(u-u_{h_2}, T-T_{h_2})\|_0^2 \\
&= A\big((u-u_{h_2}, T-T_{h_2}), (\phi-v_{h_2}, \varphi-\psi_{h_2})\big) \\
&\quad + d(u-u_{h_2}, \theta-q_{h_2}) - d(\phi-v_{h_2}, p-p_{h_2}) \\
&\quad + B\big((u_{h_1}, u_{h_1}), (u-u_{h_1}, T-T_{h_1}), (\phi-v_{h_2}, \varphi-\psi_{h_2})\big) \\
&\quad + B\big((u-u_{h_1}, u-u_{h_1}), (u, T), (\phi-v_{h_2}, \varphi-\psi_{h_2})\big) \\
&\quad - PrRa\big(i(T-T_{h_2}), \phi-v_{h_2}\big) \\
&\quad + B\big((u_{h_1}, u_{h_1}), (u_{h_1}-u_{h_2}, T_{h_1}-T_{h_2}), (\phi, \varphi)\big) \\
&\quad + B\big((u_{h_1}-u_{h_2}, u_{h_1}-u_{h_2}), (u, T), (\phi, \varphi)\big) \\
&\le C\big(h_2^2 + h_2 h_1\big)\big(\|(\phi, \varphi)\|_2 + \|\theta\|_1\big).
\end{aligned}$$

With the help of (4.8), we complete the proof. □

Thanks to the relationship of $h_j = h_{j-1}^2$ with $j \ge 3$, by the same techniques as used in Theorems 4.2-4.4, we obtain the following convergence results of numerical solution $(u_{h_j}, p_{h_j}, T_{h_j})$ in the multi-level method based on the Stokes iteration.

Theorem 4.5. *Under the assumptions of Theorem* 4.1*, the numerical solution* $(u_{h_j}, p_{h_j}, T_{h_j})$ *of problem* (4.2) *on the mesh* K_{h_j} *satisfies*

$$\begin{aligned}
&\|(u-u_{h_j}, T-T_{h_j})\|_1 + \|p-p_{h_j}\|_0 \le C\big(h_j + h_{j-1}^{\frac{3}{2}}\big) \simeq Ch_j, \quad h_j = \mathcal{O}\big(h_{j-1}^{\frac{3}{2}}\big), \\
&\|(u-u_{h_j}, T-T_{h_j})\|_0 \le C\big(h_j^2 + h_j h_{j-1}\big) \simeq Ch_j^{\frac{3}{2}}, \qquad\qquad h_j = \mathcal{O}\big(h_{j-1}^2\big).
\end{aligned}$$

5. Multi-level Method Based on the Oseen Iteration

This section considers the multi-level method based on the Oseen iteration for problem (2.1) (Algorithm 5.1).

Theorem 5.1. *Under the assumptions of Theorem* 2.1*, the numerical solutions* u_{h_j} *and* T_{h_j} *of problem* (5.1) *satisfy*

$$\begin{aligned}
&\|(u_{h_j}, T_{h_j})\|_1 \le \frac{\|F_\xi\|_{-1}}{\min\{Pr, C_0^2 PrRa\}}, \\
&\|(A_{1h}u_{h_j}, A_{2h}T_{h_j})\|_0 \le C(\|F_\xi\|_{-1} + \|F\|_0).
\end{aligned} \tag{5.2}$$

Algorithm 5.1: Multi-level Method Based on the Oseen Iteration.

Step I: *Find $(u_{h_0}, p_{h_0}, T_{h_0}) \in X_{h_0} \times M_{h_0} \times W_{h_0}$ by (4.1).

Step II: *Solve the linearized problem based on the Oseen iteration on K_{h_j} successively, i.e., for all $(v_{h_j}, q_{h_j}, \psi_{h_j}) \in X_{h_j} \times M_{h_j} \times W_{h_j}$, find $(u_{h_j}, p_{h_j}, T_{h_j}) \in X_{h_j} \times M_{h_j} \times W_{h_j}$ with $j = 1, 2, \ldots, J$ such as

$$\begin{aligned}
&A\big((u_{h_j}, T_{h_j}), (v_{h_j}, \psi_{h_j})\big) - d(v_{h_j}, p_{h_j}) + d(u_{h_j}, q_{h_j}) \\
&\quad + B\big((u_{h_{j-1}}, u_{h_{j-1}}), (u_{h_j}, T_{h_j}), (v_{h_j}, \psi_{h_j})\big) \\
&= PrRa(iT_{h_j}, v_{h_j}) + \langle F, (v_{h_j}, \psi_{h_j})\rangle.
\end{aligned} \tag{5.1}$$

Proof. We prove it by the mathematical induction. From Theorem 3.1, one knows that (5.2) holds with $j = 0$. Assume that (5.2) holds with $j = m - 1$, we prove it with $j = m$.

Choosing $(v_{h_m}, q_{h_m}, \psi_{h_m}) = (u_{h_m}, p_{h_m}, \xi T_{h_m})$ in (5.1) and using (2.3), (2.5), (2.6), one finds that

$$\begin{aligned}
&\min\{Pr, \xi k\}\|(u_{h_m}, T_{h_m})\|_1^2 \\
&\le A\big((u_{h_m}, T_{h_m}), (u_{h_m}, \xi T_{h_m})\big) \\
&= PrRa(iT_{h_m}, u_{h_m}) + \langle F, (u_{h_m}, \xi T_{h_m})\rangle \\
&\le C_0^2 PrRa\|T_{h_m}\|_1\|(u_{h_m}, T_{h_m})\|_1 + \|F_\xi\|_{-1}\|(u_{h_m}, T_{h_m})\|_1.
\end{aligned}$$

With the choice of ξ, we have

$$\min\big\{Pr, C_0^2 PrRa\big\}\|(u_{h_m}, T_{h_m})\|_1 \le \|F_\xi\|_{-1}. \tag{5.3}$$

Next, taking $v_{h_m} = A_{1h_m} u_{h_m}, q_{h_m} = 0, \psi_{h_m} = A_{2h_m} T_{h_m}$ in (5.1) and using (2.3), (2.8), one gets

$$\begin{aligned}
&\min\{Pr, k\}\|(A_{1h_m} u_{h_m}, A_{2h_m} T_{h_m})\|_0^2 \\
&\le A\big((u_{h_m}, T_{h_m}), (A_{1h_m} u_{h_m}, A_{2h_m} T_{h_m})\big) \\
&= PrRa(iT_{h_m}, A_{1h_m} u_{h_m}) + \langle F, (A_{1h_m} u_{h_m}, A_{2h_m} T_{h_m})\rangle \\
&\quad - B\big((u_{h_{m-1}}, u_{h_{m-1}}), (u_{h_m}, T_{h_m}), (A_{1h_m} u_{h_m}, A_{2h_m} T_{h_m})\big) \\
&\le PrRa\|T_{h_m}\|_0\|(A_{1h_m} u_{h_m}, A_{2h_m} T_{h_m})\|_0 + \|F\|_0\|(A_{1h_m} u_{h_m}, A_{2h_m} T_{h_m})\|_0 \\
&\quad + C_2\|(u_{h_{m-1}}, u_{h_{m-1}})\|_1\|(u_{h_m}, T_{h_m})\|_1^{\frac{1}{2}}\|(A_{1h_m} u_{h_m}, A_{2h_m} T_{h_m})\|_0^{\frac{3}{2}}.
\end{aligned}$$

As a consequence, we have

$$\begin{aligned}
&\min\{Pr, k\}\|(A_{1h_m} u_{h_m}, A_{2h_m} T_{h_m})\|_0 \\
&\le PrRa\|T_{h_m}\|_0 + \|F\|_0 + C_2\|(u_{h_{m-1}}, u_{h_{m-1}})\|_1\|(u_{h_m}, T_{h_m})\|_1^{\frac{1}{2}}\|(A_{1h_m} u_{h_m}, A_{2h_m} T_{h_m})\|_0^{\frac{1}{2}} \\
&\le C_0 PrRa\|T_{h_m}\|_1 + \|F\|_0 + \frac{C_2^2}{2\min\{Pr, k\}}\|(u_{h_{m-1}}, u_{h_{m-1}})\|_1^2\|(u_{h_m}, T_{h_m})\|_1 \\
&\quad + \frac{\min\{Pr, k\}}{2}\|(A_{1h_m} u_{h_m}, A_{2h_m} T_{h_m})\|_0.
\end{aligned} \tag{5.4}$$

Combining (5.4) with (5.3), we complete the proof. □

Theorem 5.2. *Under the assumptions of Theorem* 5.1*, the numerical solution* (u_{h_1}, T_{h_1}) *of problem* (5.1) *on the mesh* K_{h_1} *satisfies*

$$\|(u - u_{h_1}, T - T_{h_1})\|_1 + \|p - p_{h_1}\|_0 \le C\big(h_1 + h_0^2\big).$$

Proof. For all $(v_{h_1}, q_{h_1}, \psi_{h_1}) \in X_{h_1} \times M_{h_1} \times W_{h_1}$, the following error equation holds:

$$\begin{aligned}
&A\big((u - u_{h_1}, T - T_{h_1}), (v_{h_1}, \psi_{h_1})\big) - d(v_{h_1}, p - p_{h_1}) \\
&\quad + B\big((u, u), (u, T), (v_{h_1}, \psi_{h_1})\big) + d(u - u_{h_1}, q_{h_1}) \\
&\quad - B\big((u_{h_0}, u_{h_0}), (u_{h_1}, T_{h_1}), (v_{h_1}, \psi_{h_1})\big) \\
&= PrRa\big(i(T - T_{h_1}), v_{h_1}\big).
\end{aligned} \tag{5.5}$$

Taking $v_{h_1} = R_{h_1}(u,p) - u_{h_1}, q_{h_1} = Q_{h_1}(u,p) - p_{h_1}, \psi_{h_1} = \xi(\widetilde{P}_{h_1}T - T_{h_1})$ in (5.5), applying the Stokes projection, the elliptic projection, (2.5) and (2.7), one finds that

$$\begin{aligned}
&\min\{Pr, \xi k\}\big\|\big(R_{h_1}(u,p) - u_{h_1}, \widetilde{P}_{h_1}T - T_{h_1}\big)\big\|_1^2 \\
&\le A\big((R_{h_1}(u,p) - u_{h_1}, \widetilde{P}_{h_1}T - T_{h_1}), \big(R_{h_1}(u,p) - u_{h_1}, \xi(\widetilde{P}_{h_1}T - T_{h_1})\big)\big) \\
&= PrRa\big(i(T - T_{h_1}), R_{h_1}(u,p) - u_{h_1}\big) \\
&\quad - B\big((u - u_{h_0}, u - u_{h_0}), (u,T), \big(R_{h_1}(u,p) - u_{h_1}, \xi(\widetilde{P}_{h_1}T - T_{h_1})\big)\big) \\
&\quad - B\big((u_{h_0}, u_{h_0}), (u - u_{h_1}, T - T_{h_1}), \big(R_{h_1}(u,p) - u_{h_1}, \xi(\widetilde{P}_{h_1}T - T_{h_1})\big)\big) \\
&\le C_0^2 PrRa(\|T - \widetilde{P}_{h_1}T\|_1 + \|\widetilde{P}_{h_1}T - T_{h_1}\|_1)\big\|\big(R_{h_1}(u,p) - u_{h_1}, \widetilde{P}_{h_1}T - T_{h_1}\big)\big\|_1 \\
&\quad + C_1\xi\|(u - u_{h_0}, u - u_{h_0})\|_0\|(A_1u, A_2T)\|_0\big\|\big(R_{h_1}(u,p) - u_{h_1}, \widetilde{P}_{h_1}T - T_{h_1}\big)\big\|_1 \\
&\quad + C_1\xi\|(A_{1h_0}u_{h_0}, A_{1h_0}u_{h_0})\|_0\big\|\big(u - R_{h_1}(u,p), T - \widetilde{P}_{h_1}T\big)\big\|_0 \\
&\quad \times \big\|\big(R_{h_1}(u,p) - u_{h_1}, \widetilde{P}_{h_1}T - T_{h_1}\big)\big\|_1.
\end{aligned}$$

As a consequence, with the choice of ξ, (3.3) and Theorem 3.1, we have

$$\min\big\{Pr, C_0^2 PrRa\big\}\big\|\big(R_{h_1}(u,p) - u_{h_1}, \widetilde{P}_{h_1}T - T_{h_1}\big)\big\|_1 \le C\big(h_0^2 + h_1\big).$$

Thanks to the triangular inequality and the discrete inf-sup condition (3.1), we complete the proof. □

Theorem 5.3. *Under the assumptions of Theorem* 5.1*, the numerical solution* (u_{h_1}, T_{h_1}) *of problem* (5.1) *on the mesh* K_{h_1} *satisfies*

$$\|(u - u_{h_1}, T - T_{h_1})\|_0 \le C\big(h_1^2 + h_1h_0\big).$$

Proof. Setting $\widetilde{F} = (u - u_{h_1}, T - T_{h_1})$ and $(w,r,s) = (u - u_{h_1}, p - p_{h_1}, T - T_{h_1})$ in (4.7), it holds

$$\begin{aligned}
&\|(u - u_{h_1}, T - T_{h_1})\|_0^2 \\
&= A\big((\phi,\varphi), (u - u_{h_1}, T - T_{h_1})\big) - d(u - u_{h_1}, \theta) \\
&\quad + B\big((u_{h_0}, u_{h_0}), (u - u_{h_1}, T - T_{h_1}), (\phi,\varphi)\big) \\
&\quad + d(\phi, p - p_{h_1}) + B\big((u - u_{h_1}, u - u_{h_1}), (u,T), (\phi,\varphi)\big) \\
&\quad - PrRa\big(i(T - T_{h_1}), \phi\big).
\end{aligned}$$

Using the error equation (5.5), we have

$$\begin{aligned}
&\|(u - u_{h_1}, T - T_{h_1})\|_0^2 \\
&= A\big((u - u_{h_1}, T - T_{h_1}), (\phi - v_{h_1}, \varphi - \psi_{h_1})\big) \\
&\quad + d(u - u_{h_1}, \theta - q_{h_1}) - d(\phi - v_{h_1}, p - p_{h_1}) \\
&\quad + B\big((u_{h_0}, u_{h_0}), (u - u_{h_1}, T - T_{h_1}), (\phi - v_{h_1}, \varphi - \psi_{h_1})\big) \\
&\quad + B\big((u - u_{h_0}, u - u_{h_0}), (u,T), (\phi - v_{h_1}, \varphi - \psi_{h_1})\big) \\
&\quad - PrRa\big(i(T - T_{h_1}), \phi - v_{h_1}\big) \\
&\quad + B\big((u_{h_0} - u_{h_1}, u_{h_0} - u_{h_1}), (u,T), (\phi,\varphi)\big).
\end{aligned}$$

By employing the same techniques as used in Theorem 4.3 and choosing

$$(v_{h_1}, q_{h_1}, \psi_{h_1}) = (I_{h_1}\phi, \Pi_{h_1}\theta, J_{h_1}\varphi) \in X_{h_1} \times M_{h_1} \times W_{h_1},$$

we obtain

$$\|(u - u_{h_1}, T - T_{h_1})\|_0^2 \le C\big(h_1^2 + h_1 h_0\big)(\|(\phi, \varphi)\|_2 + \|\theta\|_1).$$

With the help of (4.8) and $\widetilde{F} = (u - u_{h_1}, T - T_{h_1})$, we complete the proof. □

With the relationship of $h_j = h_{j-1}^2$ as $j \ge 2$, by the same techniques as used in Theorems 4.4, the following convergence results of multi-level method based on the Oseen iteration hold.

Theorem 5.4. *Under the assumptions of Theorem* 5.1*, the numerical solution* $(u_{h_j}, p_{h_j}, T_{h_j})$ *of problem* (5.1) *on the mesh* K_{h_j} *satisfies*

$$\begin{aligned}
&\|(u - u_{h_j}, T - T_{h_j})\|_1 + \|p - p_{h_j}\|_0 \le C\big(h_j + h_{j-1}^{\frac{3}{2}}\big) \simeq Ch_j, \quad h_j = \mathcal{O}\big(h_{j-1}^{\frac{3}{2}}\big),\\
&\|(u - u_{h_j}, T - T_{h_j})\|_0 \le C\big(h_j^2 + h_j h_{j-1}\big) \simeq Ch_j^{\frac{3}{2}}, \qquad\qquad h_j = \mathcal{O}\big(h_{j-1}^2\big).
\end{aligned}$$

6. Multi-level Method Based on the Newton Iteration

In this section, we consider the multi-level method based on the Newton iteration for problem (2.1) (Algorithm 6.1).

Theorem 6.1. *Under the assumptions of Theorem* 2.1 *and* $0 < \sigma \le 1/7$*, the numerical solutions* u_{h_j} *and* T_{h_j} *of problem* (6.1) *satisfy*

$$\begin{aligned}
&\|(u_{h_j}, T_{h_j})\|_1 \le \frac{5}{3}\frac{\|F_\xi\|_{-1}}{\min\{Pr, C_0^2 PrRa\}},\\
&\|(A_{1h}u_{h_j}, A_{2h}T_{h_j})\|_0 \le C(\|F_\xi\|_{-1} + \|F\|_0).
\end{aligned} \tag{6.2}$$

Proof. We prove it by the mathematical induction. From Theorem 3.1, one knows that (6.2) holds with $j = 0$. Assume that (6.2) holds with $j = m - 1$, we prove it with $j = m$.

Algorithm 6.1: Multi-level Method Based on the Newton Iteration.

Step I: *Find $(u_{h_0}, p_{h_0}, T_{h_0}) \in X_{h_0} \times M_{h_0} \times W_{h_0}$ by (4.1).

Step II: *Solve the linearized problem based on the Newton iteration on the mesh K_{h_j} successively, i.e., for all $(v_{h_j}, q_{h_j}, \psi_{h_j}) \in X_{h_j} \times M_{h_j} \times W_{h_j}$, find $(u_{h_j}, p_{h_j}, T_{h_j}) \in X_{h_j} \times M_{h_j} \times W_{h_j}$ with $j = 1, 2, \ldots, J$ such as

$$\begin{aligned}
&A\big((u_{h_j}, T_{h_j}), (v_{h_j}, \psi_{h_j})\big) - d(v_{h_j}, p_{h_j})\\
&\quad + B\big((u_{h_{j-1}}, u_{h_{j-1}}), (u_{h_j}, T_{h_j}), (v_{h_j}, \psi_{h_j})\big)\\
&\quad + d(u_{h_j}, q_{h_j}) + B\big((u_{h_j}, T_{h_j}), (u_{h_{j-1}}, u_{h_{j-1}}), (v_{h_j}, \psi_{h_j})\big)\\
&= PrRa(iT_{h_j}, v_{h_j}) + \langle F, (v_{h_j}, \psi_{h_j})\rangle\\
&\quad + B\big((u_{h_{j-1}}, u_{h_{j-1}}), (u_{h_{j-1}}, u_{h_{j-1}}), (v_{h_j}, \psi_{h_j})\big).
\end{aligned} \tag{6.1}$$

Choosing $(v_{h_m}, q_{h_m}, \psi_{h_m}) = (u_{h_m}, p_{h_m}, \xi T_{h_m})$ in (6.1) and using (2.3), (2.5), (2.6), one gets

$$\begin{aligned}
&\min\{Pr, \xi k\}\|(u_{h_m}, T_{h_m})\|_1^2 \le A\big((u_{h_m}, T_{h_m}), (u_{h_m}, \xi T_{h_m})\big)\\
&= PrRa(iT_{h_m}, u_{h_m}) + B\big((u_{h_{m-1}}, u_{h_{m-1}}), (u_{h_{m-1}}, T_{h_{m-1}}), (u_{h_m}, \xi T_{h_m})\big)\\
&\quad + \langle F, (u_{h_m}, \xi T_{h_m})\rangle - B\big((u_{h_m}, T_{h_m}), (u_{h_{m-1}}, T_{h_{m-1}}), (u_{h_m}, \xi T_{h_m})\big)\\
&\le C_0^2 PrRa\|T_{h_m}\|_1\|(u_{h_m}, T_{h_m})\|_1 + \max\{N, \xi\bar{N}\}\|(u_{h_{m-1}}, u_{h_{m-1}})\|_1^2\|(u_{h_m}, T_{h_m})\|_1\\
&\quad + \|F_\xi\|_{-1}\|(u_{h_m}, T_{h_m})\|_1 + \max\{N, \xi\bar{N}\}\|(u_{h_{m-1}}, u_{h_{m-1}})\|_1\|(u_{h_m}, T_{h_m})\|_1^2.
\end{aligned}$$

Thanks to the condition $0 < \sigma \le 1/7$ and the choice of $\xi = 2C_0^2 PrRak^{-1}$, we have

$$\begin{aligned}
&\min\big\{Pr, C_0^2 PrRa\big\}\left(1 - \frac{1}{7}\right)\|(u_{h_m}, T_{h_m})\|_1\\
&\le \min\big\{Pr, C_0^2 PrRa\big\}(1-\sigma)\|(u_{h_m}, T_{h_m})\|_1\\
&\le \min\big\{Pr, C_0^2 PrRa\big\}\left(1 - \frac{\max\{N, \xi\bar{N}\}}{\min\{Pr, C_0^2 PrRa\}}\|(u_{h_{m-1}}, u_{h_{m-1}})\|_1\right)\|(u_{h_m}, T_{h_m})\|_1\\
&\le \|F_\xi\|_{-1} + \max\{N, \xi\bar{N}\}\|(u_{h_{m-1}}, u_{h_{m-1}})\|_1^2\\
&\le \|F_\xi\|_{-1} + \frac{25}{9}\frac{\max\{N, \xi\bar{N}\}\|F_\xi\|_{-1}}{\big(\min\big\{Pr, C_0^2 PrRa\big\}\big)^2}\|F_\xi\|_{-1}\\
&\le \left(1 + \frac{25}{9}\times\frac{1}{7}\right)\|F_\xi\|_{-1} = \frac{88}{63}\|F_\xi\|_{-1}.
\end{aligned} \tag{6.3}$$

As a consequence, we obtain the bounds of numerical solutions u_{h_m} and T_{h_m} in the H^1-norm.

Next, taking $v_{h_m} = A_{1h_m}u_{h_m}, q_{h_m} = 0, \psi_{h_m} = A_{2h_m}T_{h_m}$ in (6.1) and using (2.3), (2.8), one has

$$\begin{aligned}
&\min\{Pr, k\}\|(A_{1h_m}u_{h_m}, A_{2h_m}T_{h_m})\|_0^2 \le A\big((u_{h_m}, T_{h_m}), (A_{1h_m}u_{h_m}, A_{2h_m}T_{h_m})\big)\\
&= PrRa(iT_{h_m}, A_{1h_m}u_{h_m}) - B\big((u_{h_{m-1}}, u_{h_{m-1}}), (u_{h_m}, T_{h_m}), (A_{1h_m}u_{h_m}, A_{2h_m}T_{h_m})\big)\\
&\quad + \langle F, (A_{1h_m}u_{h_m}, A_{2h_m}T_{h_m})\rangle - B\big((u_{h_m}, T_{h_m}), (u_{h_{m-1}}, u_{h_{m-1}}), (A_{1h_m}u_{h_m}, A_{2h_m}T_{h_m})\big)\\
&\quad + B\big((u_{h_{m-1}}, u_{h_{m-1}}), (u_{h_{m-1}}, T_{h_{m-1}}), (A_{1h_m}u_{h_m}, A_{2h_m}T_{h_m})\big)\\
&\le PrRa\|T_{h_m}\|_0\|(A_{1h_m}u_{h_m}, A_{2h_m}T_{h_m})\|_0 + \|F\|_0\|(A_{1h_m}u_{h_m}, A_{2h_m}T_{h_m})\|_0\\
&\quad + 2C_2\|(u_{h_{m-1}}, u_{h_{m-1}})\|_1\|(u_{h_m}, T_{h_m})\|_1^{\frac{1}{2}}\|(A_{1h_m}u_{h_m}, A_{2h_m}T_{h_m})\|_0^{\frac{3}{2}}\\
&\quad + C_2\|(u_{h_{m-1}}, u_{h_{m-1}})\|_1^{\frac{3}{2}}\|(A_{1h_{m-1}}u_{h_{m-1}}, A_{2h_{m-1}}T_{h_{m-1}})\|_0^{\frac{1}{2}}\|(A_{1h_m}u_{h_m}, A_{2h_m}T_{h_m})\|_0.
\end{aligned}$$

As a consequence, we have

$$\begin{aligned}
&\min\{Pr, k\}\|(A_{1h_m}u_{h_m}, A_{2h_m}T_{h_m})\|_0\\
&\le PrRa\|T_{h_m}\|_0 + \|F\|_0\\
&\quad + 2C_2\|(u_{h_{m-1}}, u_{h_{m-1}})\|_1\|(u_{h_m}, T_{h_m})\|_1^{\frac{1}{2}}\|(A_{1h_m}u_{h_m}, A_{2h_m}T_{h_m})\|_0^{\frac{1}{2}}\\
&\quad + C_2\|(u_{h_{m-1}}, u_{h_{m-1}})\|_1^{\frac{3}{2}}\|(A_{1h_{m-1}}u_{h_{m-1}}, A_{2h_{m-1}}T_{h_{m-1}})\|_0^{\frac{1}{2}}.
\end{aligned}$$

If

$$\|(A_{1h_m}u_{h_m}, A_{2h_m}T_{h_m})\|_0 \le \|(A_{1h_{m-1}}u_{h_{m-1}}, A_{2h_{m-1}}T_{h_{m-1}})\|_0,$$

by the induction assumption, we get

$$\|(A_{1h_m}u_{h_m}, A_{2h_m}T_{h_m})\|_0 \le C(\|F\|_0 + \|F_\xi\|_{-1}).$$

If

$$\|(A_{1h_m}u_{h_m}, A_{2h_m}T_{h_m})\|_0 \geq \|(A_{1h_{m-1}}u_{h_{m-1}}, A_{2h_{m-1}}T_{h_{m-1}})\|_0,$$

by the Cauchy inequality, we have

$$\begin{aligned}
&\min\{Pr,k\}\|(A_{1h_m}u_{h_m}, A_{2h_m}T_{h_m})\|_0\\
&\leq C_0PrRa\|T_{h_m}\|_1 + \|F\|_0 + \frac{C_2^2}{\min\{Pr,k\}}\|(u_{h_{m-1}}, u_{h_{m-1}})\|_1^3\\
&\quad + \frac{4C_2^2}{\min\{Pr,k\}}\|(u_{h_{m-1}}, u_{h_{m-1}})\|_1^2\|(u_{h_j}, T_{h_j})\|_1\\
&\quad + \frac{\min\{Pr,k\}}{2}\|(A_{1h_m}u_{h_m}, A_{2h_m}T_{h_m})\|_0. \qquad (6.4)
\end{aligned}$$

Combining (6.4) with (6.3), we complete the proof. □

Theorem 6.2. *Under the assumptions of Theorem* 6.1*, the numerical solution* (u_{h_1}, T_{h_1}) *of problem* (6.1) *on the mesh* K_{h_1} *satisfies*

$$\|(u-u_{h_1}, T-T_{h_1})\|_1 + \|p-p_{h_1}\|_0 \leq C\big(h_1 + h_0^2\big).$$

Proof. For all $(v_{h_1}, q_{h_1}, \psi_{h_1}) \in X_{h_1} \times M_{h_1} \times W_{h_1}$, the following error equation holds:

$$\begin{aligned}
&A\big((u-u_{h_1}, T-T_{h_1}), (v_{h_1}, \psi_{h_1})\big) - d(v_{h_1}, p-p_{h_1})\\
&\quad + B\big((u,u), (u,T), (v_{h_1}, \psi_{h_1})\big)\\
&\quad + d(u-u_{h_1}, q_{h_1}) - B\big((u_{h_0}, u_{h_0}), (u_{h_1}, T_{h_1}), (v_{h_1}, \psi_{h_1})\big)\\
&\quad - B\big((u_{h_1}, T_{h_1}), (u_{h_0}, u_{h_0}), (v_{h_1}, \psi_{h_1})\big)\\
&= PrRa\big(i(T-T_{h_1}), v_{h_1}\big) - B\big((u_{h_0}, u_{h_0}), (u_{h_0}, T_{h_0}), (v_{h_1}, \psi_{h_1})\big). \qquad (6.5)
\end{aligned}$$

Taking $v_{h_1} = R_{h_1}(u,p) - u_{h_1}, q_{h_1} = Q_{h_1}(u,p) - p_{h_1}, \psi_{h_1} = \xi(\widetilde{P}_{h_1}T - T_{h_1})$ in (6.5), applying the Stokes projection, the elliptic projection, (2.5) and (2.7), one finds that

$$\begin{aligned}
&\min\{Pr,\xi k\}\big\|\big(R_{h_1}(u,p) - u_{h_1}, \widetilde{P}_{h_1}T - T_{h_1}\big)\big\|_1^2\\
&\leq A\big(\big(R_{h_1}(u,p) - u_{h_1}, \widetilde{P}_{h_1}T - T_{h_1}\big), \big(R_{h_1}(u,p) - u_{h_1}, \xi(\widetilde{P}_{h_1}T - T_{h_1})\big)\big)\\
&= PrRa\big(i(T-T_{h_1}), R_{h_1}(u,p) - u_{h_1}\big)\\
&\quad - B\big((u-u_{h_1}, u-u_{h_1}), (u_{h_0}, T_{h_0}), \big(R_{h_1}(u,p) - u_{h_1}, \xi(\widetilde{P}_{h_1}T - T_{h_1})\big)\big)\\
&\quad - B\big((u_{h_0}, u_{h_0}), (u - R_{h_1}(u,p), T - \widetilde{P}_{h_1}T), \big(R_{h_1}(u,p) - u_{h_1}, \xi(\widetilde{P}_{h_1}T - T_{h_1})\big)\big)\\
&\quad - B\big((u-u_{h_0}, u-u_{h_0}), (u-u_{h_0}, T-T_{h_0}), \big(R_{h_1}(u,p) - u_{h_1}, \xi(\widetilde{P}_{h_1}T - T_{h_1})\big)\big)\\
&\leq C_0^2PrRa(\|T - \widetilde{P}_{h_1}T\|_1 + \|\widetilde{P}_{h_1}T - T_{h_1}\|_1)\big\|\big(R_{h_1}(u,p) - u_{h_1}, \widetilde{P}_{h_1}T - T_{h_1}\big)\big\|_1\\
&\quad + \max\{N, \xi\bar{N}\}\|(u-u_{h_1}, u-u_{h_1})\|_1\|(u_{h_0}, T_{h_0})\|_1\big\|\big(R_{h_1}(u,p) - u_{h_1}, \widetilde{P}_{h_1}T - T_{h_1}\big)\big\|_1\\
&\quad + \max\{N, \xi\bar{N}\}\|(u_{h_0}, T_{h_0})\|_1\big\|\big(u - R_{h_1}(u,p), T - \widetilde{P}_{h_1}T\big)\big\|_1\\
&\quad \times \big\|\big(R_{h_1}(u,p) - u_{h_1}, \widetilde{P}_{h_1}T - T_{h_1}\big)\big\|_1\\
&\quad + \max\{N, \xi\bar{N}\}\|(u-u_{h_0}, u-u_{h_0})\|_1\|(u-u_{h_0}, T-T_{h_0})\|_1\\
&\quad \times \big\|\big(R_{h_1}(u,p) - u_{h_1}, \widetilde{P}_{h_1}T - T_{h_1}\big)\big\|_1.
\end{aligned}$$

As a consequence, with the choice of ξ, (3.3) and Theorem 6.1, we arrive at

$$\min\{Pr, C_0^2 PrRa\}\big\|\big(R_{h_1}(u,p)-u_{h_1}, \widetilde{P}_{h_1}T - T_{h_1}\big)\big\|_1 \le C\big(h_1 + h_0^2\big).$$

Thanks to the triangular inequality and the discrete inf-sup condition (3.1), we complete the proof. □

Theorem 6.3. *Under the assumptions of Theorem* 6.1*, the numerical solution* (u_{h_1}, T_{h_1}) *of problem* (6.1) *on the mesh* K_{h_1} *satisfies*

$$\|(u-u_{h_1}, T-T_{h_1})\|_0 \le C\big(h_1^2 + h_1 h_0^2 + h_0^3\big).$$

Proof. Setting $\widetilde{F} = (u-u_{h_1}, T-T_{h_1})$ and $(w,r,s) = (u-u_{h_1}, p-p_{h_1}, T-T_{h_1})$ in (4.7), it holds

$$\begin{aligned}
&\|(u-u_{h_1}, T-T_{h_1})\|_0^2 \\
&= A\big((\phi,\varphi),(u-u_{h_1}, T-T_{h_1})\big) - d(u-u_{h_1},\theta) \\
&\quad + B\big((u_{h_0},u_{h_0}),(u-u_{h_1}, T-T_{h_1})(\phi,\varphi)\big) \\
&\quad + d(\phi, p-p_{h_1}) + B\big((u-u_{h_1}, u-u_{h_1}),(u,T),(\phi,\varphi)\big) \\
&\quad - PrRa\big(i(T-T_{h_1}),\phi\big).
\end{aligned}$$

Using the error equation (6.5) and choosing $(v_{h_1}, q_{h_1}, \psi_{h_1}) \in X_{h_1} \times M_{h_1} \times W_{h_1}$, we have

$$\begin{aligned}
&\|(u-u_{h_1}, T-T_{h_1})\|_0^2 \\
&= A\big((u-u_{h_1}, T-T_{h_1}),(\phi - v_{h_1}, \varphi - \psi_{h_1})\big) \\
&\quad + d(u-u_{h_1}, \theta - q_{h_1}) - d(\phi - v_{h_1}, p - p_{h_1}) \\
&\quad - PrRa\big(i(T-T_{h_1}), \phi - v_{h_1}\big) \\
&\quad + B\big((u_{h_0},u_{h_0}),(u-u_{h_1}, T-T_{h_1}),(\phi - v_{h_1}, \varphi - \psi_{h_1})\big) \\
&\quad + B\big((u-u_{h_1}, u-u_{h_1}),(u-u_{h_0}, T-T_{h_0}),(\phi,\varphi)\big) \\
&\quad + B\big((u-u_{h_1}, u-u_{h_1}),(u_{h_0}, T_{h_0}),(\phi - v_{h_1}, \varphi - \psi_{h_1})\big) \\
&\quad + B\big((u-u_{h_0}, u-u_{h_0}),(u-u_{h_0}, T-T_{h_0}),(\phi - v_{h_1}, \varphi - \psi_{h_1})\big) \\
&\quad - B\big((u-u_{h_0}, u-u_{h_0}),(u-u_{h_0}, T-T_{h_0}),(\phi,\varphi)\big).
\end{aligned}$$

Using (2.6), (2.7) and Theorem 6.1 and choosing $(v_{h_1}, q_{h_1}, \psi_{h_1}) = (I_{h_1}\phi, \Pi_{h_1}\theta, J_{h_1}\varphi)$, we obtain

$$\|(u-u_{h_1}, T-T_{h_1})\|_0^2 \le C\big(h_1^2 + h_1 h_0^2 + h_0^3\big)(\|(\phi,\varphi)\|_2 + \|\theta\|_1).$$

With the help of (4.8) and $\widetilde{F} = (u-u_{h_1}, T-T_{h_1})$, we complete the proof. □

By the relationship of $h_j = h_{j-1}^2$ with $j \ge 2$ and the same techniques as used in Theorems 6.2 and 6.3, the following convergence results of multi-level method based on the Newton iteration hold.

Theorem 6.4. *Under the assumptions of Theorem* 6.1*, the numerical solution* $(u_{h_j}, p_{h_j}, T_{h_j})$ *of problem* (6.1) *on the mesh* K_{h_j} *satisfies*

$$\begin{aligned}
&\|(u-u_{h_j}, T-T_{h_j})\|_1 + \|p-p_{h_j}\|_0 \le C\big(h_j + h_{j-1}^2\big) \simeq Ch_j, \quad h_j = \mathcal{O}\big(h_{j-1}^2\big), \\
&\|(u-u_{h_j}, T-T_{h_j})\|_0 \le C\big(h_j^2 + h_j h_{j-1}^2 + h_{j-1}^3\big) \simeq Ch_j^{\frac{3}{2}}, \qquad h_j = \mathcal{O}\big(h_{j-1}^2\big).
\end{aligned}$$

7. Numerical Examples

In this section, we present some numerical results to verify the established theoretical findings and show the performances of the considered numerical methods. The stable MINI element is used to approximate the velocity and pressure, and the linear polynomial is adopted for the temperature field.

7.1. Convergence validation with the analytical solution

In this test, our purpose is to verify the theoretical findings which have been established in Sections 4-6 by setting the physical parameters $Pr = 10, Ra = k = 1$. The body forces f and g are given by the following exact solution:

$$\begin{aligned}
&u_1 = 10x^2(x-1)^2y(y-1)(2y-1),\\
&u_2 = -10x(x-1)(2x-1)y^2(y-1)^2,\\
&p = 10(2x-1)(2y-1),\\
&T = 10x(x-1)y(y-1)\big(x(x-1)(2y-1) - (2x-1)y(y-1)\big).
\end{aligned}$$

Case 1. The domain $\Omega = [0,1]^2$.

Firstly, we test the numerical examples in a square area Ω, the regular partitions of Ω into the triangles. Table 7.1 presents the numerical results obtained by the standard Galerkin FEM (3.4) for the Boussinesq equations with different mesh sizes. From these data, one can see that the relative errors of numerical approximations become smaller and smaller as mesh size decreases, and the convergence rates of numerical solutions are all optimal, i.e., the convergence orders of velocity and temperature in L^2- and H^1-norms are 2 and 1, respectively.

Table 7.1: The numerical results of Galerkin method in the square area.

$\frac{1}{h}$	$\frac{\|u-u_h\|_0}{\|u\|_0}$	u_{L^2} rate	$\frac{\|\nabla(u-u_h)\|_0}{\|\nabla u\|_0}$	u_{H^1} rate	$\frac{\|p-p_h\|_0}{\|p\|_0}$	p_{L^2} rate
9	0.091458		0.308605		0.017019	
16	0.0288694	2.00412	0.16828	1.054	0.00652057	1.66741
25	0.0117372	2.01669	0.106371	1.02781	0.00311878	1.65257
36	0.0056304	2.01452	0.0734391	1.01599	0.0017355	1.60744
49	0.00302826	2.01165	0.0537846	1.01027	0.00106754	1.5762
64	0.00177069	2.00933	0.0411003	1.00715	0.000704521	1.55616
81	0.00110347	2.00757	0.0324339	1.00528	0.0004898	1.54318
$\frac{1}{h}$	$\frac{\|T-T_h\|_0}{\|T\|_0}$	T_{L^2} rate	$\frac{\|\nabla(T-T_h)\|_0}{\|\nabla T\|_0}$	T_{H^1} rate	CPU time (S)	
9	0.0547535		0.236979		0.283	
16	0.0175445	1.97806	0.134454	0.985032	0.845	
25	0.00721297	1.99167	0.0862612	0.994518	2.329	
36	0.00348324	1.99625	0.0599569	0.997562	4.474	
49	0.00188128	1.99808	0.0440668	0.998758	8.196	
64	0.00110309	1.99892	0.0337449	0.999303	14.701	
81	0.000688758	1.99935	0.0266653	0.999579	23.324	

Next, we show the performances of the multi-level methods (4.2), (5.1) and (6.1) based on different iterations. Tables 7.2-7.7 give the numerical results of two-level and three-level

Table 7.2: The numerical results of two level method based on Stokes iteration in the square area.

$\frac{1}{h_0}$	$\frac{1}{h_1}$	$\frac{\|u-u_h\|_0}{\|u\|_0}$	u_{L^2} rate	$\frac{\|\nabla(u-u_h)\|_0}{\|\nabla u\|_0}$	u_{H^1} rate	$\frac{\|p-p_h\|_0}{\|p\|_0}$	p_{L^2} rate
3	9	0.0915525		0.308613		0.0170149	
4	16	0.0289074	2.00363	0.168281	1.05403	0.00652094	1.66689
5	25	0.0117525	2.01671	0.106371	1.02782	0.00312069	1.65133
6	36	0.0056421	2.01240	0.0734393	1.01599	0.00173775	1.60557
7	49	0.00303644	2.00963	0.0537847	1.01028	0.00106978	1.57359
8	64	0.00177652	2.00712	0.0411003	1.00715	0.000706652	1.55271
9	81	0.0011078	2.00489	0.032434	1.00528	0.000491787	1.53882
$\frac{1}{h_0}$	$\frac{1}{h_1}$	$\frac{\|T-T_h\|_0}{\|T\|_0}$	T_{L^2} rate	$\frac{\|\nabla(T-T_h)\|_0}{\|\nabla T\|_0}$	T_{H^1} rate	CPU time (S)	
3	9	0.0548016		0.23699		0.135	
4	16	0.0176269	1.97143	0.134463	0.984984	0.338	
5	25	0.00730068	1.9751	0.0862683	0.994493	0.744	
6	36	0.00357811	1.9557	0.0599623	0.997537	1.473	
7	49	0.00197963	1.91996	0.0440711	0.998741	2.718	
8	64	0.00120308	1.86482	0.0337483	0.999289	4.760	
9	81	0.00078824	1.79498	0.026668	0.99957	7.720	

Table 7.3: The numerical results of two level method based on Oseen iteration in the square area.

$\frac{1}{h_0}$	$\frac{1}{h_1}$	$\frac{\|u-u_h\|_0}{\|u\|_0}$	u_{L^2} rate	$\frac{\|\nabla(u-u_h)\|_0}{\|\nabla u\|_0}$	u_{H^1} rate	$\frac{\|p-p_h\|_0}{\|p\|_0}$	p_{L^2} rate
3	9	0.0914539		0.30861		0.0170191	
4	16	0.0288694	2.00404	0.168281	1.05402	0.00652126	1.66723
5	25	0.0117386	2.01641	0.106371	1.02781	0.00311958	1.65223
6	36	0.00563519	2.01252	0.0734392	1.01599	0.00173627	1.60694
7	49	0.00303238	2.00999	0.0537847	1.01027	0.00106821	1.57558
8	64	0.00177396	2.00753	0.0411003	1.00715	0.000705125	1.55531
9	81	0.00110608	2.00533	0.032434	1.00528	0.000490343	1.54211
$\frac{1}{h_0}$	$\frac{1}{h_1}$	$\frac{\|T-T_h\|_0}{\|T\|_0}$	T_{L^2} rate	$\frac{\|\nabla(T-T_h)\|_0}{\|\nabla T\|_0}$	T_{H^1} rate	CPU time (S)	
3	16	0.0547355		0.236985		0.141	
4	16	0.017583	1.97367	0.134459	0.985002	0.339	
5	25	0.00725586	1.98331	0.086265	0.994512	0.779	
6	36	0.0035306	1.97547	0.0599597	0.997554	1.559	
7	49	0.00193031	1.95843	0.0440689	0.998754	2.868	
8	64	0.00115306	1.92936	0.0337466	0.999299	5.026	
9	81	0.000738644	1.89059	0.0266666	0.999577	8.012	

Table 7.4: The numerical results of two level method based on Newton iteration in the square area.

$\frac{1}{h_0}$	$\frac{1}{h_1}$	$\frac{\|u-u_h\|_0}{\|u\|_0}$	u_{L^2} rate	$\frac{\|\nabla(u-u_h)\|_0}{\|\nabla u\|_0}$	u_{H^1} rate	$\frac{\|p-p_h\|_0}{\|p\|_0}$	p_{L^2} rate
3	9	0.0914034		0.308608		0.0170210	
4	16	0.0288298	2.00546	0.168280	1.05402	0.0065216	1.66734
5	25	0.0117208	2.01675	0.106371	1.02781	0.0031192	1.65262
6	36	0.0056235	2.01404	0.0734391	1.01599	0.00173568	1.60754
7	49	0.0030247	2.01147	0.0537846	1.01027	0.00106762	1.57626
8	64	0.0017686	2.00927	0.0411003	1.00715	0.000704564	1.55622
9	81	0.0011022	2.00754	0.0324339	1.00528	0.000489825	1.54323
$\frac{1}{h_0}$	$\frac{1}{h_1}$	$\frac{\|T-T_h\|_0}{\|T\|_0}$	T_{L^2} rate	$\frac{\|\nabla(T-T_h)\|_0}{\|\nabla T\|_0}$	T_{H^1} rate	CPU time (S)	
3	9	0.0547085		0.23698		0.16	
4	16	0.017533	1.97777	0.134454	0.985034	0.408	
5	25	0.00720796	1.99176	0.0862613	0.994522	0.942	
6	36	0.00348082	1.99625	0.0599569	0.997564	1.89	
7	49	0.00187997	1.99809	0.0440668	0.998759	3.412	
8	64	0.00110233	1.99888	0.033745	0.999304	6.482	
9	81	0.00068829	1.99932	0.0266653	0.999579	9.606	

Table 7.5: The numerical results of three level method based on Stokes iteration in the square area.

$\frac{1}{h_0}$	$\frac{1}{h_1}$	$\frac{1}{h_2}$	$\frac{\|u-u_h\|_0}{\|u\|_0}$	u_{L^2} rate	$\frac{\|\nabla(u-u_h)\|_0}{\|\nabla u\|_0}$	u_{H^1} rate	$\frac{\|p-p_h\|_0}{\|p\|_0}$	p_{L^2} rate
2	3	9	0.0915524		0.308613		0.0170149	
2	4	16	0.0289073	2.00363	0.168281	1.05403	0.00652094	1.66689
2	5	25	0.0117523	2.01673	0.106371	1.02782	0.00312069	1.65133
2	6	36	0.00564201	2.01241	0.0734393	1.01599	0.00173775	1.60557
2	7	49	0.00303636	2.00966	0.0537847	1.01028	0.00106978	1.57358
2	8	64	0.00177645	2.00718	0.0411003	1.00715	0.000706654	1.5527
3	9	81	0.00110772	2.00499	0.032434	1.00528	0.000491789	1.53881
$\frac{1}{h_0}$	$\frac{1}{h_1}$	$\frac{1}{h_2}$	$\frac{\|T-T_h\|_0}{\|T\|_0}$	T_{L^2} rate	$\frac{\|\nabla(T-T_h)\|_0}{\|\nabla T\|_0}$	T_{H^1} rate	CPU time (S)	
2	3	9	0.054801		0.23699		0.111	
2	4	16	0.017625	1.97161	0.134463	0.984984	0.295	
2	5	25	0.00729733	1.97588	0.0862683	0.994493	0.674	
2	6	36	0.00357371	1.95781	0.0599624	0.997537	1.445	
2	7	49	0.00197452	1.92435	0.0440711	0.998741	2.979	
2	8	64	0.00119761	1.8722	0.0337483	0.999289	4.220	
3	9	81	0.000782636	1.80594	0.026668	0.999569	6.897	

methods. From these data, one can see that the convergence rates of various numerical solutions are all optimal in the considered numerical schemes. While the multi-level method based on the Stokes iteration costs the least CPU time, and the multi-level method based on the Newton

Table 7.6: The numerical results of three level method based on Oseen iteration in the square area.

$\frac{1}{h_0}$	$\frac{1}{h_1}$	$\frac{1}{h_2}$	$\frac{\|u-u_h\|_0}{\|u\|_0}$	u_{L^2} rate	$\frac{\|\nabla(u-u_h)\|_0}{\|\nabla u\|_0}$	u_{H^1} rate	$\frac{\|p-p_h\|_0}{\|p\|_0}$	p_{L^2} rate
2	3	9	0.0914538		0.30861		0.0170191	
2	4	16	0.0288693	2.00404	0.168281	1.05402	0.00652126	1.66724
2	5	25	0.0117386	2.01642	0.106371	1.02781	0.00311958	1.65223
2	6	36	0.00563515	2.01253	0.0734392	1.01599	0.00173627	1.60695
2	7	49	0.00303236	2.00999	0.0537847	1.01027	0.00106821	1.57558
2	8	64	0.00177394	2.00754	0.0411003	1.00715	0.00070512	1.55533
3	9	81	0.00110607	2.00534	0.032434	1.00528	0.000490338	1.54213
$\frac{1}{h_0}$	$\frac{1}{h_1}$	$\frac{1}{h_2}$	$\frac{\|T-T_h\|_0}{\|T\|_0}$	T_{L^2} rate	$\frac{\|\nabla(T-T_h)\|_0}{\|\nabla T\|_0}$	T_{H^1} rate	CPU time (S)	
2	3	9	0.0547355		0.236985		0.12	
2	4	16	0.017583	1.97367	0.134459	0.985001	0.331	
2	5	25	0.00725578	1.98333	0.0862649	0.994512	0.723	
2	6	36	0.00353046	1.97555	0.0599597	0.997554	1.491	
2	7	49	0.00193011	1.95864	0.0440689	0.998754	2.662	
2	8	64	0.00115275	1.92997	0.0337466	0.9993	4.665	
3	9	81	0.000738266	1.89163	0.0266666	0.999578	7.768	

Table 7.7: The numerical results of three level method based on Newton iteration in the square area.

$\frac{1}{h_0}$	$\frac{1}{h_1}$	$\frac{1}{h_2}$	$\frac{\|u-u_h\|_0}{\|u\|_0}$	u_{L^2} rate	$\frac{\|\nabla(u-u_h)\|_0}{\|\nabla u\|_0}$	u_{H^1} rate	$\frac{\|p-p_h\|_0}{\|p\|_0}$	p_{L^2} rate
2	3	9	0.0914034		0.308608		0.017021	
2	4	16	0.0288298	2.00547	0.16828	1.05402	0.00652161	1.66734
2	5	25	0.0117207	2.01675	0.106371	1.02781	0.0031192	1.65262
2	6	36	0.00562351	2.01403	0.0734391	1.01599	0.00173568	1.60754
2	7	49	0.00302471	2.01148	0.0537846	1.01027	0.00106762	1.57626
2	8	64	0.00176864	2.00928	0.0411003	1.00715	0.000704564	1.55622
3	9	81	0.00110219	2.00755	0.0324339	1.00528	0.000489825	1.54323
$\frac{1}{h_0}$	$\frac{1}{h_1}$	$\frac{1}{h_2}$	$\frac{\|T-T_h\|_0}{\|T\|_0}$	T_{L^2} rate	$\frac{\|\nabla(T-T_h)\|_0}{\|\nabla T\|_0}$	T_{H^1} rate	CPU time (S)	
2	3	9	0.0547079		0.23698		0.147	
2	4	16	0.0175322	1.97783	0.134454	0.985034	0.381	
2	5	25	0.00720711	1.99192	0.0862613	0.994522	0.855	
2	6	36	0.00348003	1.99655	0.0599569	0.997564	1.751	
2	7	49	0.00187931	1.99848	0.0440668	0.998759	3.131	
2	8	64	0.00110178	1.99946	0.033745	0.999304	5.592	
3	9	81	0.000687831	2.00002	0.0266653	0.999579	9.032	

iteration has the highest accuracy. Tables 7.8-7.10 compare the numerical results of two-level and three-level methods at the same fine mesh size. From these tables, one finds that almost the same numerical results are obtained by using the two-level and three-level methods, while

Table 7.8: The numerical results of j-level method based on Stokes iteration in the square area.

$\frac{1}{h_0}$-$\frac{1}{h_1}$-$\frac{1}{h_2}$	$\frac{\|u-u_h\|_0}{\|u\|_0}$	$\frac{\|\nabla(u-u_h)\|_0}{\|\nabla u\|_0}$	$\frac{\|p-p_h\|_0}{\|p\|_0}$	$\frac{\|T-T_h\|_0}{\|T\|_0}$	$\frac{\|\nabla(T-T_h)\|_0}{\|\nabla T\|_0}$	CPU time (S)
8-16	0.02890	0.16828	0.006520	0.01789	0.134497	0.385
4-8-16	0.02887	0.16828	0.006520	0.01755	0.134455	0.317
16-32	0.007167	0.08275	0.002094	0.005661	0.0675251	1.514
4-16-32	0.007138	0.08275	0.002094	0.004405	0.0674367	1.203
32-64	0.001800	0.04110	0.0007046	0.003738	0.0339223	6.043
16-32-64	0.001771	0.04110	0.0007045	0.001103	0.033745	4.799
64-128	0.0004700	0.02049	0.0002433	0.003586	0.0172281	26.479
32-64-128	0.0004408	0.02049	0.0002431	0.0002759	0.0168758	22.628

Table 7.9: The numerical results of j-level method based on Oseen iteration in the square area.

$\frac{1}{h_0}$-$\frac{1}{h_1}$-$\frac{1}{h_2}$	$\frac{\|u-u_h\|_0}{\|u\|_0}$	$\frac{\|\nabla(u-u_h)\|_0}{\|\nabla u\|_0}$	$\frac{\|p-p_h\|_0}{\|p\|_0}$	$\frac{\|T-T_h\|_0}{\|T\|_0}$	$\frac{\|\nabla(T-T_h)\|_0}{\|\nabla T\|_0}$	CPU time (S)
8-16	0.02887	0.1683	0.006521	0.01755	0.1345	0.39
4-8-16	0.02887	0.1683	0.006521	0.01755	0.1345	0.307
16-32	0.007138	0.08275	0.002094	0.004408	0.06744	1.411
4-16-32	0.007138	0.08275	0.002094	0.004408	0.06744	1.162
32-64	0.001771	0.04110	0.0007045	0.001103	0.03375	6.471
16-32-64	0.001771	0.04110	0.0007045	0.001103	0.03375	5.052
64-128	0.0004408	0.02049	0.0002431	0.0002759	0.01688	29.48
32-64-128	0.0004408	0.02049	0.0002431	0.0002759	0.01688	22.931

Table 7.10: The numerical results of j-level method based on Newton iteration in the square area.

$\frac{1}{h_0}$-$\frac{1}{h_1}$-$\frac{1}{h_2}$	$\frac{\|u-u_h\|_0}{\|u\|_0}$	$\frac{\|\nabla(u-u_h)\|_0}{\|\nabla u\|_0}$	$\frac{\|p-p_h\|_0}{\|p\|_0}$	$\frac{\|T-T_h\|_0}{\|T\|_0}$	$\frac{\|\nabla(T-T_h)\|_0}{\|\nabla T\|_0}$	CPU time (S)
8-16	0.02887	0.1683	0.006521	0.01755	0.1345	0.434
4-8-16	0.02887	0.1683	0.006521	0.01754	0.1345	0.38
16-32	0.007138	0.0828	0.002094	0.004408	0.06744	1.686
4-16-32	0.007137	0.0828	0.002094	0.004407	0.06744	1.368
32-64	0.001771	0.04110	0.0007045	0.001103	0.03375	7.033
16-32-64	0.001771	0.04110	0.0007045	0.001103	0.03374	6.417
64-128	0.0004408	0.02049	0.0002431	0.0002759	0.01688	32.222
32-64-128	0.0004408	0.02049	0.0002431	0.0002759	0.01688	25.865

the three-level method takes less CPU time than two-level method. Moreover, the convergence orders of variables in both L^2- and H^1-norms are all optimal.

Case 2. The L-shape domain $\Omega = [-1,1]^2 - [-1,0]^2$.

Now, we consider the computational efficiency of multi-level method in a L-shape domain. Fig. 7.1 shows the domain and the corresponding boundary conditions.

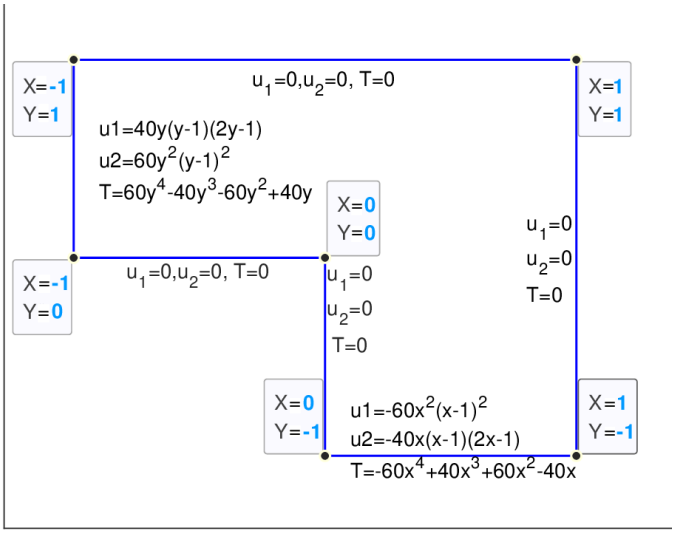

Fig. 7.1. The L-shape domain and the boundary conditions.

Table 7.11: The numerical results of Galerkin method in the L-shape domain.

$\frac{1}{h}$	$\frac{\|u-u_h\|_0}{\|u\|_0}$	u_{L^2} rate	$\frac{\|\nabla(u-u_h)\|_0}{\|\nabla u\|_0}$	u_{H^1} rate	$\frac{\|p-p_h\|_0}{\|p\|_0}$	p_{L^2} rate
9	0.0640448		0.301366		4.44892	
16	0.0203579	1.9919	0.152313	1.18601	1.67219	1.70071
25	0.00836208	1.9937	0.0945068	1.06942	0.729457	1.85887
36	0.0039983	2.0234	0.0615563	1.17573	0.428215	1.46081
49	0.00214293	2.023	0.0446058	1.04472	0.236287	1.92856
64	0.00125086	2.0158	0.033482	1.07411	0.151289	1.66948
81	0.000784337	1.9813	0.0269079	0.92793	0.108916	1.39502
$\frac{1}{h}$	$\frac{\|T-T_h\|_0}{\|T\|_0}$	T_{L^2} rate	$\frac{\|\nabla(T-T_h)\|_0}{\|\nabla T\|_0}$	T_{H^1} rate	CPU time (S)	
9	0.0400799		0.236348		1.26	
16	0.0120316	2.09144	0.133284	0.99559	3.876	
25	0.00547596	1.76381	0.0897762	0.88543	10.373	
36	0.00240024	2.26194	0.0590876	1.14715	21.353	
49	0.00130072	1.98717	0.0440836	0.95015	41.323	
64	0.000758842	2.01781	0.0334312	1.03571	71.826	
81	0.000484542	1.90431	0.0270127	0.90497	119.079	

Table 7.11 presents the numerical results obtained by the Galerkin FEM (3.4) for the Boussinesq equations with different mesh sizes in the L-shape domain. From these data, one can see that the relative errors of (u_h, p_h, T_h) decrease as the mesh size refines, and the convergence rates of numerical solutions are all optimal. Tables 7.12-7.14 present the numerical results of two-level method with the Stokes, Oseen and Newton iterations. From these data, we find that the convergence rates of numerical solution (u_h, p_h, T_h) are optimal in the corresponding

Table 7.12: The numerical results of two level method based on Stokes iteration in L-shape domain.

$\frac{1}{h_0}$	$\frac{1}{h_1}$	$\frac{\|u-u_h\|_0}{\|u\|_0}$	u_{L^2} rate	$\frac{\|\nabla(u-u_h)\|_0}{\|\nabla u\|_0}$	u_{H^1} rate	$\frac{\|p-p_h\|_0}{\|p\|_0}$	p_{L^2} rate
3	9	0.0640849		0.301371		4.44621	
4	16	0.0203758	1.99154	0.152323	1.18592	1.67312	1.69868
5	25	0.0083878	1.98879	0.0945108	1.06947	0.731121	1.85501
6	36	0.00402066	2.01658	0.0615608	1.17564	0.430136	1.45479
7	49	0.00215825	2.01799	0.0446105	1.04461	0.238614	1.91129
8	64	0.00126443	2.00206	0.0334863	1.07403	0.153524	1.65125
9	81	0.000798072	1.95351	0.0269104	0.92806	0.110948	1.37879
$\frac{1}{h_0}$	$\frac{1}{h_1}$	$\frac{\|T-T_h\|_0}{\|T\|_0}$	T_{L^2} rate	$\frac{\|\nabla(T-T_h)\|_0}{\|\nabla T\|_0}$	T_{H^1} rate	CPU time (S)	
3	9	0.260096		0.131056		0.477	
4	16	0.148155	1.10538	0.0693819	0.97814	1.294	
5	25	0.0995999	0.78842	0.0488016	0.88978	2.77	
6	36	0.0663275	1.02433	0.0335906	1.11494	5.315	
7	49	0.0495272	1.01905	0.0245343	0.94739	10.085	
8	64	0.0379857	0.87234	0.0194355	0.99344	17.312	
9	81	0.0305765	0.87454	0.0158171	0.92110	28.401	

Table 7.13: The numerical results of two level method based on Oseen iteration in L-shape domain.

$\frac{1}{h_0}$	$\frac{1}{h_1}$	$\frac{\|u-u_h\|_0}{\|u\|_0}$	u_{L^2} rate	$\frac{\|\nabla(u-u_h)\|_0}{\|\nabla u\|_0}$	u_{H^1} rate	$\frac{\|p-p_h\|_0}{\|p\|_0}$	p_{L^2} rate
3	9	0.0640627		0.301369		4.44653	
4	16	0.020371	1.99135	0.152316	1.18599	1.672	1.69997
5	25	0.00837184	1.99252	0.0945075	1.06944	0.72965	1.85803
6	36	0.00401108	2.0179	0.061557	1.17571	0.428738	1.45819
7	49	0.00214944	2.02352	0.0446064	1.04471	0.236925	1.92377
8	64	0.00126071	1.99778	0.0334825	1.0741	0.151935	1.66361
9	81	0.00079204	1.97319	0.0269082	0.92794	0.109541	1.3888
$\frac{1}{h_0}$	$\frac{1}{h_1}$	$\frac{\|T-T_h\|_0}{\|T\|_0}$	T_{L^2} rate	$\frac{\|\nabla(T-T_h)\|_0}{\|\nabla T\|_0}$	T_{H^1} rate	CPU time (S)	
3	9	0.102823		0.248811		0.434	
4	16	0.0562056	1.04975	0.141134	0.98543	1.161	
5	25	0.0345121	1.09281	0.0943439	0.90247	2.663	
6	36	0.0241989	0.97356	0.0624612	1.13097	5.476	
7	49	0.017471	1.05665	0.0464845	0.95824	10.503	
8	64	0.0134247	0.98644	0.0352633	1.0345	17.355	
9	81	0.01084	0.90785	0.0284759	0.90753	29.364	

numerical schemes except the L^2-errors of temperature, the reason is the poor approximations of the corner on the coarse mesh. Tables 7.15-7.17 show the three-level methods based on the different iterations. From these tables, one finds that the desired convergence orders of T in L^2-norm are achieved with the refined coarse mesh sizes.

Table 7.14: The numerical results of two level method based on Newton iteration in L-shape domain.

$\frac{1}{h_0}$	$\frac{1}{h_1}$	$\frac{\|u-u_h\|_0}{\|u\|_0}$	u_{L^2} rate	$\frac{\|\nabla(u-u_h)\|_0}{\|\nabla u\|_0}$	u_{H^1} rate	$\frac{\|p-p_h\|_0}{\|p\|_0}$	p_{L^2} rate
3	9	0.0640539		0.301368		4.44768	
4	16	0.0203588	1.99215	0.152314	1.18601	1.67229	1.70012
5	25	0.00836539	1.99291	0.0945073	1.06942	0.729387	1.85922
6	36	0.00399997	2.02339	0.0615564	1.17573	0.428144	1.46101
7	49	0.00214278	2.02458	0.0446059	1.04472	0.236289	1.92799
8	64	0.0012507	2.016	0.0334821	1.07412	0.151303	1.66916
9	81	0.000784556	1.97968	0.0269079	0.92793	0.108914	1.39547
$\frac{1}{h_0}$	$\frac{1}{h_1}$	$\frac{\|T-T_h\|_0}{\|T\|_0}$	T_{L^2} rate	$\frac{\|\nabla(T-T_h)\|_0}{\|\nabla T\|_0}$	T_{H^1} rate	CPU time (S)	
3	9	0.0610805		0.239866		0.502	
4	16	0.0164478	2.2803	0.133851	1.01389	1.37	
5	25	0.00807063	1.59529	0.0900068	0.88920	3.258	
6	36	0.00352358	2.27278	0.0591664	1.15052	6.385	
7	49	0.00176743	2.23791	0.0441138	0.95225	11.974	
8	64	0.000918521	2.4508	0.0334396	1.03734	20.546	
9	81	0.000680092	1.27581	0.0270187	0.9051	33.905	

Table 7.15: The numerical results of three level method based on Stokes iteration in L-shape domain.

$\frac{1}{h_0}$	$\frac{1}{h_1}$	$\frac{1}{h_2}$	$\frac{\|u-u_h\|_0}{\|u\|_0}$	u_{L^2} rate	$\frac{\|\nabla(u-u_h)\|_0}{\|\nabla u\|_0}$	u_{H^1} rate	$\frac{\|p-p_h\|_0}{\|p\|_0}$	p_{L^2} rate
3	6	9	0.0640486		0.301366		4.44818	
3	8	16	0.0203516	1.99262	0.152314	1.186	1.67177	1.70085
3	10	25	0.00836443	1.99238	0.0945072	1.0694	0.729573	1.85795
3	12	36	0.00399771	2.02463	0.0615566	1.1757	0.42834	1.46045
$\frac{1}{h_0}$	$\frac{1}{h_1}$	$\frac{1}{h_2}$	$\frac{\|T-T_h\|_0}{\|T\|_0}$	T_{L^2} rate	$\frac{\|\nabla(T-T_h)\|_0}{\|\nabla T\|_0}$	T_{H^1} rate	CPU time (S)	
3	6	9	0.0514505 (0.0514505)		0.238564		0.569	
3(8)	8(12)	16	0.0221209 (0.0149179)	1.4670(2.1517)	0.134889	0.99099	1.278	
3(15)	10(20)	25	0.0141106 (0.0063056)	1.0074(1.9295)	0.0912085	0.8768	2.696	
3(24)	12(30)	36	0.0101021 (0.0027890)	0.9164(2.2371)	0.0606096	1.12081	5.376	

7.2. Thermal driven cavity problem

In this test, we consider a benchmark problem: the thermal driven cavity model. The considered domain $\Omega = [0,1]^2$ with differentially heated vertical walls where the left and right walls are kept at T_l and T_r, respectively, with $T_l > T_r$. The remaining walls are insulated and there is no heat transfer through them. The boundary conditions are no-slip boundary conditions for the velocity at four walls ($u = 0$) and Dirichlet boundary conditions for the temperature at vertical walls. As the horizontal walls are adiabatic with $\partial T/\partial n = 0$. Fig. 7.2 shows the physical domain of the thermal driven cavity flow problem. In this test, we follow the parameters set in $[6, 25]$ and take $k = 1, f = g = 0, T_l = 1$ and $T_r = 0$. While we consider the air as the cavity filling fluid in our model, we take the fixed value $Pr = 0.71$. We perform

Table 7.16: The numerical results of three level method based on Oseen iteration in L-shape domain.

$\frac{1}{h_0}$	$\frac{1}{h_1}$	$\frac{1}{h_2}$	$\frac{\|u-u_h\|_0}{\|u\|_0}$	u_{L^2} rate	$\frac{\|\nabla(u-u_h)\|_0}{\|\nabla u\|_0}$	u_{H^1} rate	$\frac{\|p-p_h\|_0}{\|p\|_0}$	p_{L^2} rate
3	6	9	0.0640482		0.301366		4.44834	
3	8	16	0.0203617	1.99175	0.152313	1.18601	1.67194	1.70074
3	10	25	0.00836429	1.99352	0.0945069	1.06942	0.729347	1.85887
3	12	36	0.00400071	2.02252	0.0615563	1.17573	0.428166	1.46071
$\frac{1}{h_0}$	$\frac{1}{h_1}$	$\frac{1}{h_2}$	$\frac{\|T-T_h\|_0}{\|T\|_0}$	T_{L^2} rate	$\frac{\|\nabla(T-T_h)\|_0}{\|\nabla T\|_0}$	T_{H^1} rate	CPU time (S)	
3	6	9	0.0465423		0.237251		0.61	
3	8	16	0.0184118	1.6118	0.133822	0.99521	1.431	
3	10	25	0.010567	1.2441	0.0901144	0.88603	3.035	
3	12	36	0.00670356	1.2480	0.0593254	1.14644	6.027	

Table 7.17: The numerical results of three level method based on Newton iteration in L-shape domain.

$\frac{1}{h_0}$	$\frac{1}{h_1}$	$\frac{1}{h_2}$	$\frac{\|u-u_h\|_0}{\|u\|_0}$	u_{L^2} rate	$\frac{\|\nabla(u-u_h)\|_0}{\|\nabla u\|_0}$	u_{H^1} rate	$\frac{\|p-p_h\|_0}{\|p\|_0}$	p_{L^2} rate
3	6	9	0.0640461		0.301366		4.44883	
3	8	16	0.0203575	1.99205	0.152313	1.18601	1.67218	1.70068
3	10	25	0.00836209	1.99365	0.0945068	1.06942	0.72946	1.85885
3	12	36	0.00399832	2.02344	0.0615563	1.17573	0.428212	1.46084
$\frac{1}{h_0}$	$\frac{1}{h_1}$	$\frac{1}{h_2}$	$\frac{\|T-T_h\|_0}{\|T\|_0}$	T_{L^2} rate	$\frac{\|\nabla(T-T_h)\|_0}{\|\nabla T\|_0}$	T_{H^1} rate	CPU time (S)	
3	6	9	0.040379		0.2364		0.723	
3	8	16	0.0120194	2.10612	0.133289	0.99590	1.611	
3	10	25	0.00545406	1.77053	0.0897791	0.88545	3.515	
3	12	36	0.00239322	2.25898	0.0590886	1.14719	7.034	

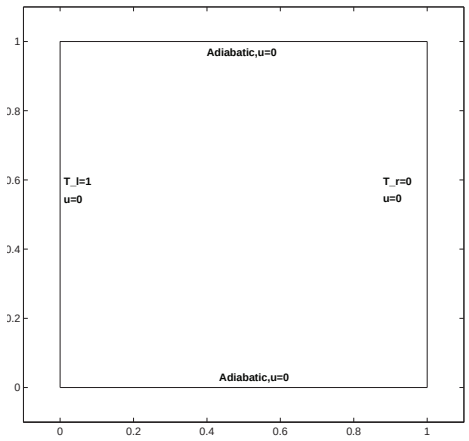

Fig. 7.2. The physical domain with its boundary conditions.

our computations for Rayleigh number varying from 10^3 to 10^5. The performances of one-level, two-level and three level methods are compared with the works [6, 25, 26, 31] on the fine mesh $h = 1/64$.

We start our illustrations by giving peak values of vertical velocity at $x = 0.5$ and horizontal velocity at $y = 0.5$. Table 7.18 summarizes the maximum vertical velocity values at mid-height and at mid-width for different Rayleigh numbers. For quantitative assessment, we also present the values obtained by [6, 25, 26, 31]. As it can be observed, as the Rayleigh number takes $10^3, 10^4$ and 10^5, the results of multi-level methods are in agreement with the benchmark data even at the coarser grid $h_0 = 1/3$. On the other hand, we compare the CPU time of multi-level methods in Table 7.18. One finds that the two-level and three level methods just take at most 25% computational cost than one-level method. Furthermore, as the Ra increase, the CPU time of one-level method increases significantly, while the CPU time of two-level and three-level methods is nearly a constant. The reasons may lie in (1) the condition number becomes worse and worse with the Ra increases, more iterative steps are needed when one solves the nonlinear problem. (2) As the Ra increases, the assembly of the Jacobians requires more computational cost. (3) The zero initial guess is not sufficient enough as a good initial guess, especially for the high value of Ra, more iterations are needed to achieve the tolerable error. Therefore the

Table 7.18: Comparisons of maximum velocity at y=0.5 and x=0.5 with different methods ($h = 1/64$).

	One-level method	Two-level method	Three-level method	
Ra=10^3	$h_0 = \frac{1}{64}$	h_0-$h_1 = \frac{1}{8}$-$\frac{1}{64}$	h_0-h_1-$h_2 = \frac{1}{3}$-$\frac{1}{8}$-$\frac{1}{64}$	
x=0.5	3.65	3.65	3.63	
y=0.5	3.70	3.69	3.69	
CPU(s)	33.27	8.05	7.54	
Ra=10^4	$h_0 = \frac{1}{64}$	h_0-$h_1 = \frac{1}{8}$-$\frac{1}{64}$	h_0-h_1-$h_2 = \frac{1}{3}$-$\frac{1}{8}$-$\frac{1}{64}$	
x=0.5	16.18	16.18	15.63	
y=0.5	19.63	19.63	19.05	
CPU(s)	47.03	8.21	7.85	
Ra=10^5	$h_0 = \frac{1}{64}$	h_0-$h_1 = \frac{1}{8}$-$\frac{1}{64}$	h_0-h_1-$h_2 = \frac{1}{3}$-$\frac{1}{8}$-$\frac{1}{64}$	
x=0.5	34.72	34.82	32.76	
y=0.5	68.47	68.54	67.86	
CPU(s)	82.97	9.39	8.71	
	Ref. [25]	Ref. [26]	Ref. [6]	Ref. [31]
Ra=10^3				
x=0.5	3.68	–	3.65	3.489
y=0.5	3.73	3.692	3.70	3.686
Ra=10^4				
x=0.5	16.10	–	16.18	16.122
y=0.5	19.90	19.63	19.51	19.79
Ra=10^5				
x=0.5	34.00	–	34.81	33.39
y=0.5	70.00	68.85	68.22	70.63

CPU time of the one-level method grows significantly. For the multi-level method, the nonlinear problem is only solved on the initial mesh and the computational scales have not changed much, as a consequence, the computational cost of multi-level method is almost the same.

Next, we compare the vertical velocity distribution at the mid-height and horizontal velocity distribution at the mid-width in Figs. 7.3-7.4 at different Rayleigh numbers with different numerical schemes, which are very popular graphical illustrations in the study of thermal driven cavity problem. It is obvious that as the Rayleigh numbers increase, the differences in the profiles are getting larger. These profiles are also comparable with the results provided in [25, 26, 31]. Combining with Table 7.18, we can say that the multi-level methods have good performances.

Finally, we show the streamlines, isobars and isotherms of the Boussinesq equations with one-level, two-level and three-level methods at different Rayleigh numbers. We present these patterns in Figs. 7.5-7.7. It is clear from the streamline pattern that, as Rayleigh number increases circular vortex at the cavity center begin to deform into an ellipse and then break up into two vortices tending to approach to the corners differentially heated sides of the cavity. Therefore, we can conclude that, the flow is faster as the thermal convection is concentrated. As the increase of Rayleigh numbers, the parallel behavior of temperature isolines is distorted as these lines seem to have a flat behavior in the central part of the region. Near the sides of the cavity, isolines tend to be vertical only. The temperature slops with $Ra = 10^5$ at the corners of the differentially heated sides are more immersed than the case of lower Rayleigh number. There is no differences of the results obtained by the one-level, two-level and three-level methods in both values and the trends of fields. We also note that these graphics are also perfectly comparable with the investigations of [6, 25, 26, 31]. Both the results and the graphics show the efficiency and effectiveness of the multi-level methods.

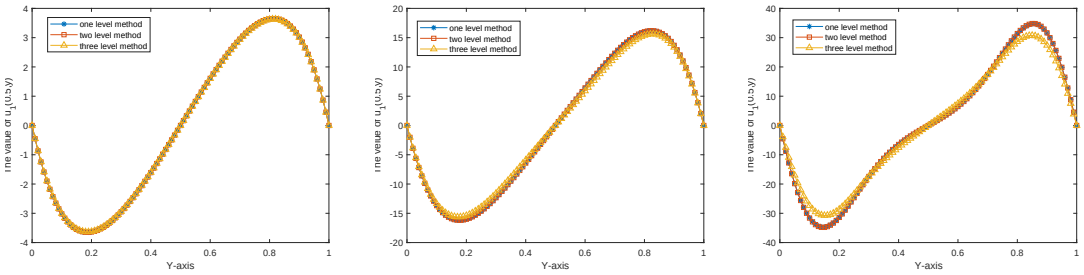

Fig. 7.3. Comparison of the value $u_1(x, y)$ at the mid-width ($x = 0.5$) with one-level, two-level and three-level methods. (a) $Ra = 10^3$, (b) $Ra = 10^4$, (c) $Ra = 10^5$.

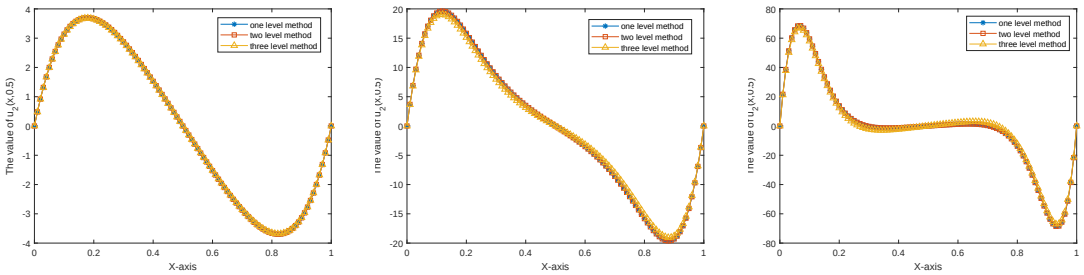

Fig. 7.4. Comparison of the value $u_2(x, y)$ at the mid-width ($y = 0.5$) with one-level, two-level and three-level methods. (a) $Ra = 10^3$, (b) $Ra = 10^4$, (c) $Ra = 10^5$.

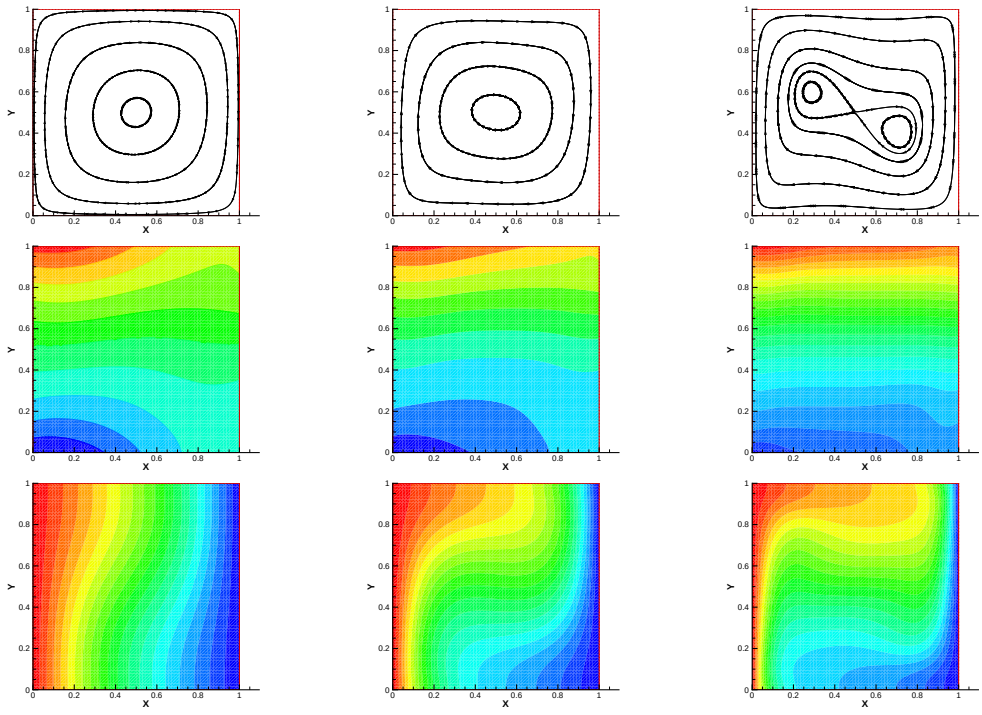

Fig. 7.5. The streamlines, isobars and isotherms obtained by the one-level method with $Ra = 10^3$ (the first column), $Ra = 10^4$ (the second column) and $Ra = 10^5$ (the third column).

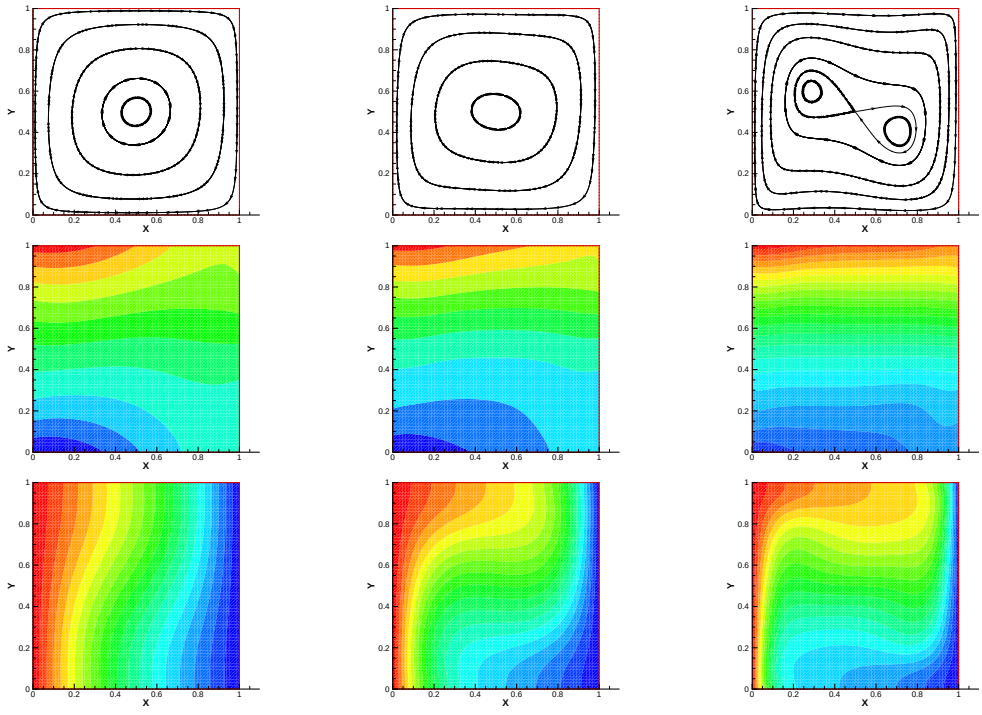

Fig. 7.6. The streamlines, isobars and isotherms obtained by the two-level method with $Ra = 10^3$ (the first column), $Ra = 10^4$ (the second column) and $Ra = 10^5$ (the third column).

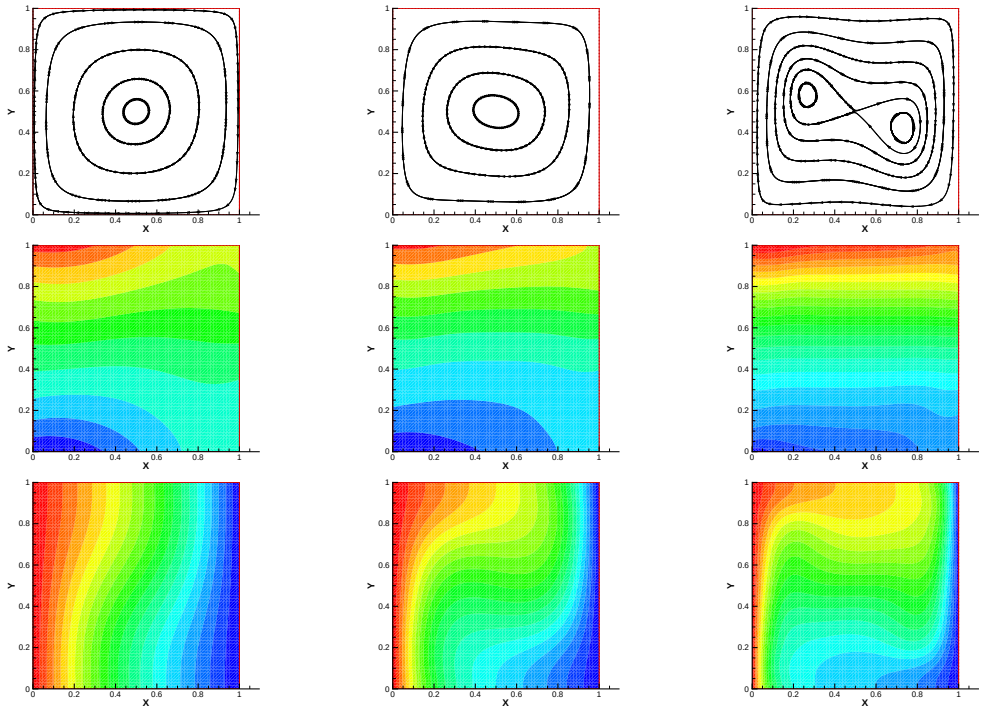

Fig. 7.7. The streamlines, isobars and isotherms obtained by the three-level method with $Ra = 10^3$ (the first column), $Ra = 10^4$ (the second column) and $Ra = 10^5$ (the third column).

8. Conclusion

In this paper, the multi-level mixed finite element methods for the steady Boussinesq equations are designed and analyzed. Firstly, some regularity results are provided by introducing suitable parameter ξ. Then, the multi-level methods based on three iterations are presented, the priori boundedness of numerical solutions are provided by using the mathematical induction. The error estimates in L^2- and H^1-norms of the multi-level methods are also obtained with the energy method and the constructed dual problems. Unfortunately, from the view of theoretical findings, the optimal convergence rates ($h_j = h_{j-1}^2$) of numerical solutions are not established due to the loss of $1/2$ in L^2-norm of numerical approximations. How to utilize the regularity of the solution (ϕ, φ) in the dual problem sufficiently to provide a new estimate of (4.9), and establish the optimal error estimates of multi-level methods will be our next goals.

Acknowledgements. This work was supported by the National Natural Science Foundation of China (Grant No. 12271468) and by the Shandong Province Natural Science Foundation (Grant No. ZR2025MS85).

References

[1] A. Barth, A. Lang, and C. Schwab, Multilevel Monte Carlo method for parabolic stochastic partial differential equations, *BIT*, **53** (2013), 3–27.

[2] A. Barth, C. Schwab, and N. Zollinger, Multi-level Monte Carlo finite element method for elliptic PDEs with stochastic coefficients, *Numer. Math.*, **119**:1 (2011), 123–161.

[3] J. Boland and W. Layton, Error analysis for finite element methods for steady natural convection problems, *Numer. Funct. Anal. Optim.*, **11** (1990), 449–483.

[4] F. Brezzi and M. Fortin, *Mixed and Hybrid Finite Element Methods*, in: *Springer Series in Computational Mathematics*, Springer-Verlag, 1991.

[5] X.C. Cai, Multiplicative Schwarz methods for parabolic problems, *SIAM J. Sci. Comput.*, **15**:3 (1994), 587–603.

[6] D. de Vahl Davis, Natural convection of air in a square cavity: A benchmark solution, *Int. J. Numer. Methods Fluids*, **3** (1983), 249–264.

[7] M. Dryja, M.V. Sarkis, and O.B. Widlund, Multilevel Schwarz methods for elliptic problems with discontinuous coefficients in three dimensions, *Numer. Math.*, **72**:3 (1996), 313–348.

[8] D.Y. Fang, W.J. Le, and T. Zhang, The 2D regularized incompressible Boussinesq equations with general critical dissipations, *J. Math. Anal. Appl.*, **46**:1 (2018), 868–915.

[9] V. Girault and P. Raviart, *Finite Element Methods for Navier-Stokes Equations*, in: *Series in Computational Mathematics*, Springer-Verlag, 1986.

[10] E. Haber and J. Modersitzki, A multilevel method for image registration, *SIAM J. Sci. Comput.*, **27**:5 (2006), 1594–1607.

[11] Y.N. He and J. Li, Convergence of three iterative methods based on the finite element discretization for the stationary Navier-Stokes equations, *Comput. Methods Appl. Mech. Engrg.*, **198** (2009), 1351–1359.

[12] R. Hiptmair and K. Neymeyr, Multilevel method for mixed eigenproblems, *SIAM J. Sci. Comput.*, **23**:6 (2002), 2141–2164.

[13] P.Z. Huang, An efficient two-level finite element algorithm for the natural convection equations, *Appl. Numer. Math.*, **118** (2017), 75–86.

[14] Q.S. Jiu, Y.Q. Wang, and G. Wu, Partial regularity of the suitable weak solutions to the multi-dimensional incompressible Boussinesq equations, *J. Dyn. Differ. Equations*, **28** (2016), 567–591.

[15] M. Ilicak, A. Ecder, and E. Turan, Operator splitting techniques for the numerical analysis of natural convection heat transfer, *Int. J. Comput. Math.*, **84**:6 (2007), 783–793.

[16] J. Lang, *Adaptive multilevel solution of nonlinear parabolic PDE systems: Theory, algorithm, and applications*, Springer-Verlag, 2001.

[17] W. Layton, H.K. Lee, and J. Peterson, Numerical solution of the stationary Navier-Stokes equations using a multilevel finite element method, *SIAM J. Sci. Comput.*, **20**:1 (1998), 1–12.

[18] W. Layton and H.W.J. Lenferink, Two-level Picard and modified Picard methods for the Navier-Stokes equations, *Appl. Math. Comput.*, **69**:2-3 (1995), 263–274.

[19] W. Layton and H.W.J. Lenferink, A multilevel mesh independence principle for the Navier-Stokes equations, *SIAM J. Numer. Anal.*, **33**:1 (1996), 17–30.

[20] W. Layton and L. Tobiska, A two-level method with backtracking for the Navier-Stokes equations, *SIAM J. Numer. Anal.*, **35**:5 (1998), 2035–2054.

[21] J. Li and Y.N. He, A multi-level discontinuous Galerkin method for solving the stationary Navier-Stokes equations, *Nonlinear Anal.*, **67** (2007), 1403–1411.

[22] J. Li, Y.N. He, and H. Xu, A multi-level stabilized finite element method for the stationary Navier-Stokes equations, *Comput. Methods Appl. Mech. Engrg.*, **196** (2007), 2852–2862.

[23] R. Lteif, An operator-splitting approach with a hybrid finite volume/finite difference scheme for extended Boussinesq models, *Appl. Numer. Math.*, **196** (2024), 159–182.

[24] Z.D. Luo, *The Bases and Applications of Mixed Finite Element Methods*, Science Press, 2006. (In Chinese)

[25] M.T. Manzari, An explicit finite element algorithm for convective heat transfer problems, *Int. J. Numer. Methods Heat Fluid Flow*, **9** (1999), 860–877.

[26] N. Massarotti, P. Nithiarasu, and O.C. Zienkiewicz, Characteristic-Based-Split (CBS) algorithm for incompressible flow problems with hear transfer, *Int. J. Numer. Methods Heat Fluid Flow*, **8** (1998), 969–990.

[27] H.L. Qiu, Multi-level mixed finite element algorithms for the stationary incompressible magneto-hydrodynamics equations, *Comput. Math. Appl.*, **86** (2021), 33–48.
[28] Z.Y. Si, Y.Q. Shang, and T. Zhang, New one- and two-level Newton iterative mixed finite element methods for stationary conduction-nonvection problems, *Finite Elem. Anal. Des.*, **47** (2011), 175–183.
[29] R. Temam, *Navier-Stokes Equations, Theory and Numerical Analysis*, North-Holland, 1984.
[30] O.V. Vasilyev and N.K.R. Kevlahan, An adaptive multilevel wavelet collocation method for elliptic problems, *J. Comput. Phys.*, **206**:2 (2005), 412–431.
[31] D.C. Wan, B.S.V. Patnaik, and G.W. Wei, A new benchmark quality solution for the buoyancy driven cavity by discrete singular convolution, *Numer. Heat Transf. B: Fundam.*, **40** (2001), 199–228.
[32] L. Wang, J. Li, and P.Z. Huang, An efficient iterative algorithm for the natural convection equations based on finite element method, *Int. J. Numer. Methods Heat Fluid Flow*, **28**:3 (2018), 584–605.
[33] S. Wang, Global well-posedness of a new class of initial-boundary value problem on incompressible MHD/MHD-Boussinesq equations, *J. Differential Equationss*, **363** (2023), 465–490.
[34] S. Wang, Y.X. Wang, and J.T. Liu, Regularity criteria to the incompressible axisymmetric Boussinesq equations, *Appl. Math. Lett.*, **112** (2021), 106800.
[35] W.L. Wang, J.L. Wu, and X.L. Feng, A novel characteristic variational multiscale FEM for incompressible natural convection problem with variable density, *Int. J. Numer. Methods Heat Fluid Flow*, **29**:2 (2019), 580–601.
[36] J. Wu and Q. Zhang, Stability and optimal decay for a system of 3D anisotropic Boussinesq equations, *Nonlinearity*, **34**:8 (2021), 5456–5484.
[37] J.C. Xu, A novel two-grid method for semi-linear elliptic equations, *SIAM J. Sci. Comput.*, **15** (1994), 231–237.
[38] J.C. Xu, Two-grid discretization techniques for linear and nonlinear PDEs, *SIAM J. Numer. Anal.*, **33** (1996), 1759–1777.
[39] W.R. Yang, Q.S. Jiu, and J.H. Wu, The 3D incompressible Boussinesq equations with fractional pratial dissipation, *Commun. Math. Sci.*, **16**:3 (2018), 617–633.
[40] Y.B. Yang, B.C. Huang, and Y.L. Jiang, Error estimates of an operator-splitting finite element method for the time-dependent natural convection problem, *Numer. Methods Partial Differential Equations*, **39**:3 (2023), 2202–2226.
[41] H.F. Zhang, C.J. Chen, and T. Zhang, Two-level iterative finite element methods for the stationary natural convection equations with different viscosities based on three corrections, *Comput. Appl. Math.*, **42** (2023), 11.
[42] T. Zhang, T. Jiang, and J.Y. Yuan, One-level and two-level finite element methods for the Boussinesq problem, *Math. Methods Appl. Sci.*, **41**:7 (2018), 2748–2768.
[43] T. Zhang and Y.X. Qian, The time viscosity-splitting method for the Boussinesq problem, *J. Math. Anal. Appl.*, **445**:1 (2017), 186–211.
[44] T. Zhang, J.Y. Yuan, and Z.Y. Si, Decoupling two grid finite element method for the non-steady natural convection problem I: Space discretization, *Numer. Methods Partial Differential Equations*, **31** (2015), 2135–2168.
[45] T. Zhang, X. Zhao, and P.Z. Huang, Decoupled two level finite element methods for the steady natural convection problem, *Numer. Algorithms*, **68** (2015), 837–866.